High-spin states with seniority $v = 4$, 5, and 6 in $^{119-126}$Sn

A. Astier,[1] M.-G. Porquet,[1] Ch. Theisen,[2] D. Verney,[3] I. Deloncle,[1] M. Houry,[2,*] R. Lucas,[2] F. Azaiez,[4,†] G. Barreau,[5] D. Curien,[4] O. Dorvaux,[4] G. Duchêne,[4] B. J. P. Gall,[4] N. Redon,[6] M. Rousseau,[4] and O. Stézowski[6]

[1]*CSNSM, IN2P3-CNRS and Université Paris-Sud, Bât 104-108, F-91405 Orsay, France*

[2]*CEA, Centre de Saclay, IRFU/Service de Physique Nucléaire, F-91191 Gif-sur-Yvette Cedex, France*

[3]*IPNO, IN2P3-CNRS and Université Paris-Sud, F-91406 Orsay, France*

[4]*IPHC, IN2P3-CNRS and Université Louis Pasteur, F-67037 Strasbourg Cedex 2, France*

[5]*CENBG, IN2P3-CNRS and Université Bordeaux I, F-33175 Gradignan, France*

[6]*IPNL, IN2P3-CNRS and Université Claude Bernard, F-69622 Villeurbanne Cedex, France*

(Received 1 December 2011; published 24 May 2012)

The $^{119-126}$Sn nuclei have been produced as fission fragments in two reactions induced by heavy ions: $^{12}C + ^{238}U$ at a bombarding energy of 90 MeV and $^{18}O + ^{208}Pb$ at 85 MeV. Their level schemes have been built from γ rays detected using the Euroball array. High-spin states located above the long-lived isomeric states of the even- and odd-A $^{120-126}$Sn nuclei have been identified. Moreover, isomeric states lying around 4.5 MeV have been established in ^{120,122,124,126}Sn from the delayed coincidences between the fission fragment detector SAPhIR and the Euroball array. The states located above 3 MeV excitation energy are ascribed to several broken pairs of neutrons occupying the $\nu h_{11/2}$ orbit. The maximum value of angular momentum available in such a high-j shell, i.e., for midoccupation and the breaking of the three neutron pairs, has been identified. This process is observed for the first time in spherical nuclei.

DOI: 10.1103/PhysRevC.85.054316 PACS number(s): 25.70.Jj, 27.60.+j, 23.20.−g, 21.60.Cs

I. INTRODUCTION

Experimental and theoretical investigations of the structure of the $_{50}$Sn nuclei have been the subject of much interest during the past few decades. Their low-lying states are textbook examples of shell-model approaches, as their description only involves excitations of a few neutrons, all along the chain of known isotopes, $^{101-134}$Sn.

The high-spin states of ^{A}Sn nuclei with $A < 120$ can be populated by fusion-evaporation reactions induced by heavy ions. Such experiments, performed many years ago, mainly led to the identification of collective rotational bands up to spin $\sim 20\hbar$ [1]. These bands are built on "intruder" configurations, i.e., two-particle–two-hole excitations across the $Z = 50$ closed shell. At mid neutron shell, this configuration is low in energy, and thus the collective rotational band, being yrast in the mass range 110–118, dominates the high-spin level schemes. Since this is no longer the case for $A \geqslant 120$, the yrast states of the heavy Sn isotopes are expected to be only due to excitations of neutrons moving in a spherical well, particularly the states due to the breaking of several pairs in the $\nu h_{11/2}$ orbit. Unfortunately, because of the lack of suitable stable projectile-target combinations, high-spin states of heavy Sn isotopes cannot be populated by fusion-evaporation reactions. Thus, up to now, medium-spin states of the $^{120-126}$Sn isotopes were only measured up to spin $I^{\pi} = 10^{+}$ for even mass and $I^{\pi} = 27/2^{-}$ for odd mass, by using reactions induced by light ions, deep inelastic reactions, isomeric decays of long-lived states of Sn produced by fission of actinides, or β decays of the high-spin long-lived states of heavy In [2–8]. During the completion of the present work, the decay of a new isomeric state in ^{128}Sn populated in the fragmentation of ^{136}Xe has been reported [9], and this has been proposed to be the 15^{-} state expected from the $(\nu h_{11/2})^{-3}(\nu d_{3/2})^{-1}$ configuration.

For the studies presented in this paper, the $^{119-126}$Sn isotopes have been produced as fragments of binary fission induced by heavy ions. We have selected two fusion-fission reactions in order to identify unambiguously the γ rays emitted by the high-spin states of these nuclei. Moreover, γ-γ angular correlations have been analyzed in order to assign spin and parity values to most of these states. In addition, new isomeric states lying around 4.5 MeV have been established in ^{120,122,124,126}Sn from the delayed coincidences between fission fragment detectors and the γ array. All the observed states can be described in terms of broken neutron pairs occupying the $\nu h_{11/2}$ orbit. The maximum value of angular momentum available in this high-j shell, i.e., for midoccupation and the breaking of the three pairs, has been identified.

II. EXPERIMENTAL METHODS AND DATA ANALYSIS

A. Reactions and γ-ray detection

The $^{12}C + ^{238}U$ reaction was studied at 90 MeV incident energy. The beam was provided by the Legnaro XTU tandem accelerator. The 47 mg/cm^2 target of ^{238}U was thick enough to stop the recoiling nuclei. The second reaction, $^{18}O + ^{208}Pb$ at 85 MeV beam energy, was studied at the Vivitron accelerator of IReS (Strasbourg). The thickness of the target was 100 mg/cm^2. In these two experiments, the γ rays were detected with the Euroball array consisting of 71 Compton-suppressed Ge detectors [10] (15 cluster germanium detectors placed in the backward hemisphere with respect to the beam, 26 clover germanium detectors located around 90°,

*Present address: CEA/DSM/Département de recherches sur la Fusion Contrôlée, F-130108 Saint-Paul lez Durance, France.

†Present address: IPNO, IN2P3-CNRS and Université Paris-Sud, F-91406 Orsay, France.

and 30 tapered single-crystal germanium detectors located at forward angles). Each cluster detector is composed of seven closely packed large-volume Ge crystals [11] and each clover detector consists of four smaller Ge crystals [12]. The data were recorded in an event-by-event mode with the requirement that a minimum of five (three) unsuppressed Ge detectors fired in prompt coincidence (within a time window of 50 ns) during the first (second) experiment. About 1.9×10^9 (4×10^9) coincidence events (within a time window of 300 ns) with a γ multiplicity greater than or equal to three were registered. The offline analysis consisted of both multigated spectra and several three-dimensional "cubes" built and analyzed with the RADWARE package [13].

B. Isomer selection

To identify new isomeric states in fission fragments, we have performed another experiment using a fission fragment detector to trigger the Euroball array and isolate the delayed γ-ray cascades. The heavy-ion detector SAPhIR (Saclay Aquitaine Photovoltaic cells for Isomer Research) is made of many photovoltaic cells which can be arranged in several geometries [14]. In the present work, it consisted of 32 photovoltaic modules laying in four rings around the target. We have used the $^{12}C + ^{238}U$ reaction at 90 MeV with a thin target, 0.14 mg/cm^2. Fragments escaping from the target are stopped in the photovoltaic cells of SAPhIR. The detection of the two fragments in coincidence provides a clean signature of fission events. The Euroball time window was 50 ns–1μs, allowing detection of delayed γ rays emitted during the de-excitation of isomeric states.

Time spectra between fragments and γ rays were analyzed in order to measure the half-life of isomeric levels. The full width at half maximum (FWHM) of the time distribution for prompt γ rays was around 15 ns. In this experiment, new isomeric states were found in ^{120,122,124}Sn nuclei, which will be detailed below.

C. Identification of new γ-ray cascades

The fusion-fission channel of the above-mentioned reactions leads to the production of the high-spin states of ~150 fragments, mainly located on the neutron-rich side of the valley of stability. This gives several thousands of γ transitions which have to be sorted out. Single-gated spectra are useless in the majority of cases. The selection of one particular nucleus needs at least two energy conditions, implying that at least two transitions have to be known.

The identification of transitions depopulating high-spin levels which are completely unknown is based on the fact that *prompt* γ rays emitted by complementary fragments are detected in coincidence [15,16]. For each reaction used in this work, we have studied the intensities of γ rays emitted by many pairs of complementary fragments with known cascades to establish the relationship between their number of protons and neutrons. The sum of the proton numbers of complementary fragments has been found to be the atomic number of the compound nucleus,[1] so that the $_{50}$Sn isotopes are associated with the $_{48}$Cd isotopes in the $^{12}C + ^{238}U$ reaction and with the $_{40}$Zr isotopes in the $^{18}O + ^{208}Pb$ reaction. The number of evaporated neutrons (sum of the pre- and post-fission emitted neutrons) extends from 7 to 14 in the first reaction [17,18] and from 2 to 7 in the second one [19,20]. The distribution and the mean number of emitted neutrons depends slightly on the N/Z ratio of the investigated fragments and on the angular momentum of their excited states emitting the γ rays. Primary fragments populated at high excitation energy cool predominantly by neutron evaporation, then the secondary fragments emit γ rays. Therefore the number of emitted neutron must be low in order to observe γ-ray cascades in the most neutron-rich isotopes.

Many new γ-ray cascades of the $^{120–126}$Sn nuclei have been identified using the distribution of masses of their partners, as explained below. It is worth noting that the use of two different reactions to produce the various Sn isotopes has turned out to be essential to disentangle the coincidence relationships, which are often complicated by the existence of many doublets or triplets of transitions very close in energy.

The relative intensity of the lowest transitions in the new cascades identified in $^{120–126}$Sn have been measured in the spectra in double coincidences with one new transition and one transition of a partner. As for the other transitions, we have used spectra in double coincidences with two transitions of the new cascades. A loss in intensity occurs when going through an isomeric state. By knowing that the time window was 300 ns for the two experiments, such an effect has been taken into account for the half-lives in the 100- to 300-ns range, observed in the present work.

D. γ-γ angular correlations

In order to determine the spin values of excited states, the coincidence rates of two successive γ transitions are analyzed as a function of θ, the average relative angle between the two fired detectors. The Euroball spectrometer had $C^2_{239} = 28441$ combinations of two crystals, out of which only ~2000 involved different values of relative angle within 2°. Therefore, in order to keep reasonable numbers of counts, all the angles have been gathered around three average relative angles: 22°, 46°, and 75°.

The coincidence rate is increasing between 0° and 90° for the dipole-quadrupole cascades, whereas it decreases for the quadrupole-quadrupole or dipole-dipole ones. More precisely, the angular correlation functions at the three angles of interest were calculated for several combinations of spin sequences, corresponding to typical multipole orders (see Table I). In order to check the method, angular correlations of transitions belonging to the yrast cascades of the fission fragments having well-known multipole orders were analyzed and the expected values were found in all cases.

[1] In the $^{12}C + ^{238}_{92}U$ reaction, we have also identified a weak exit channel: Few pairs of fragments having $Z_1 + Z_2 = 94$, instead of 98, indicates a fission process occurring after the transfer of a few nucleons.

TABLE I. Values of the angular correlation functions, $R(\theta)$, normalized to the ones calculated at 75°, computed for several combinations of spin sequences and multipole orders (Q = quadrupole and D = dipole).

Spin sequence I_1–I_2–I_3	Multipole orders	$R(22°)$	$R(46°)$	$R(75°)$
14–12–10	Q–Q	1.13	1.06	1.00
12–11–10	D–D	1.06	1.03	1.00
13–12–10	D–Q	0.92	0.96	1.00

When the statistics of our data are too low to perform such a measurement, the spin assignments are based upon (i) the already known spins of some states, (ii) the assumption that, in yrast decays, spin values increase with the excitation energy, (iii) the possible existence of crossover transitions, and (iv) the analogy with the level structures of the other isotopes.

III. EXPERIMENTAL RESULTS

The γ rays emitted by the low-lying states of $^{118-126}$Sn isotopes have been observed in both fusion-fission reactions used in the present work. As for ^{118}Sn, its yield is so low that only the decay of its 7^- state is observed and the transitions of its partners could not be identified. On the other hand, we have measured many new γ rays emitted by the high-spin states of $^{119-126}$Sn, the results of which are presented in the three following sections.

A. New γ-ray cascades of $^{120-126}$Sn isotopes

Up to now, the high-spin level schemes of $^{120-126}$Sn isotopes could only be established up to the long-lived isomeric states, with $I^\pi = 10^+$ or $27/2^-$ at about 2–3 MeV excitation energy, since it is difficult to register coincidence relationships between the transitions populating and depopulating states having such half-life values ($T_{1/2} = 1$–62μs) using standard experimental apparatus. On the other hand, in the fusion-fission experiments, all the γ-ray cascades located above the long-lived isomeric states of the Sn isotopes are easily detected in prompt coincidences with those emitted by their complementary fragments. Three steps are necessary to carry out the search:

(i) Find all the γ rays emitted in prompt coincidences with the transitions of the $^{114-122}$Cd fragments in the first data set and the $^{96-100}$Zr fragments in the second one, which do not belong to their respective level schemes.
(ii) Build all the γ-ray cascades using their own coincidences.
(iii) Assign each γ-ray cascade to one particular Sn isotope, from the distribution of masses of their partners.

The first item is illustrated in Fig. 1(a), gated by the first two transitions of ^{118}Cd (487 and 676 keV), built from the data set of the ^{12}C + ^{238}U reaction. Besides two transitions already known in ^{118}Cd in the 950- to 1250-keV energy range, a lot of new transitions are observed and can be assigned to $^{120-125}$Sn, half of them being known to belong to the cascades built on

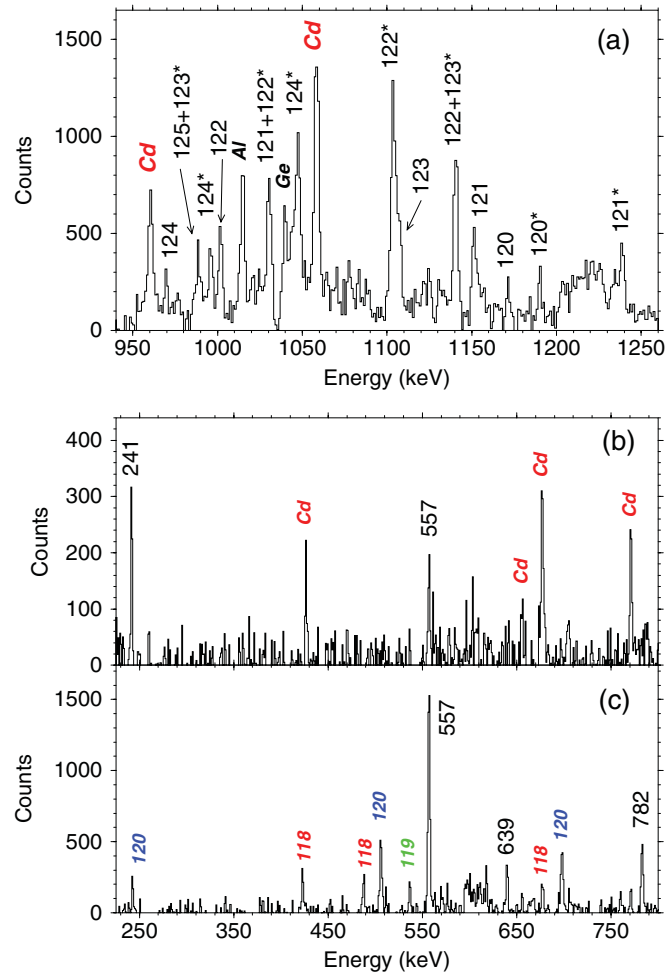

FIG. 1. (Color online) (a) Spectrum of γ rays detected in coincidence with the first two transitions of ^{118}Cd (487 and 676 keV), built from the data set of the ^{12}C + ^{238}U reaction, in the 950- to 1250-keV energy range. All the transitions but two, emitted by ^{118}Cd, belong to its complementary fragments, $^{120-125}$Sn. They are labeled by their mass A, an asterisk being added when the transition belongs to a new cascade located above a long-lived isomeric state. (b) Spectrum of γ rays detected in coincidence with the first transition of ^{118}Cd (487 keV) and the new transition at 1190 keV. Transitions emitted by ^{118}Cd are labeled by Cd. (c) Spectrum of γ rays detected in coincidence with the two new transitions at 1190 and 241 keV. Transitions emitted by the $^{118-120}$Cd complementary fragments are labeled by their mass.

their ground state (labeled by their mass A). Then in order to find the γ-ray cascades comprising the other transitions, all the spectra in double coincidence with one transition of ^{118}Cd and one new transition are precisely analyzed. For instance, in Fig. 1(b), two new γ lines at 241 and 557 keV are found to be correlated to the new 1190-keV transition and the 487-keV γ ray of ^{118}Cd. Finally, Fig. 1(c) allows us to complete the search of a new γ-ray cascade: It comprises five transitions at 1190, 557, 241, 782, and 639 keV. In addition, the fact that this third spectrum shows the transitions emitted by several Cd complementary fragments confirms that this cascade belongs to the level scheme of one Sn isotope. Using

the same procedure for each Cd isotope in the first experiment, as well as for $^{96-100}$Zr in the second one, several new γ-ray cascades have been observed in the present work.

To assign every γ-ray cascade to one particular Sn isotope, we have first analyzed the relative intensities of γ rays emitted by the partners in each spectrum in double coincidence with two transitions of the new cascades [such as the spectrum shown in Fig. 1(c)]. Then we have analyzed all these distributions of masses of the partners. Examples of results obtained in the first experiment are shown in Fig. 2. The evolution of the Cd yields from the top drawing to the bottom one proves that the six cascades belong to different Sn isotopes. Similar results are obtained from the evolution of the Zr yields associated with each cascade in the second experiment. Finally, these relative distributions of Cd and Zr masses were compared to well-known pairs of complementary fragments and the six new cascades discussed in Fig. 2 were assigned to ^{120,121,122,123,124,126}Sn. Their first transitions are marked with an asterisk in the spectrum of Fig. 1(a). Their precise locations in the Sn level schemes are discussed in the next sections.

B. Study of the even-A $^{120-126}$Sn isotopes

Very few medium-spin levels were known in the even-A $^{120-126}$Sn isotopes prior to this work. Populated in deep inelastic reactions [4,6], two long-lived isomeric states were identified from their γ decays to the low-lying states. Lying between 2 and 3 MeV excitation energy, these isomeric states are due to the breaking of one neutron pair, the state with $I^\pi = 10^+$ being attributed to a $(\nu h_{11/2})^2$ configuration and the one with $I^\pi = 7^-$ to a $(\nu h_{11/2})(\nu d_{3/2})$ configuration. Using the data of the two fusion-fission reactions of the present work, we have identified the yrast structures of $^{120-126}$Sn located above their long-lived isomeric states. In the following, we first present the building of each high-spin level scheme and the measurement of isomeric states in the 30- to 300-ns range. Then, we discuss the angular momentum and parity assignments of most of the new states of $^{120-126}$Sn.

1. ^{120}Sn

A cascade starting with the 1190- and 557-keV transitions is assigned to ^{120}Sn, because of the mass distribution of its complementary fragments in the two fusion reactions (Sec. III A). Besides the three other transitions shown in Figs. 1(b) and 1(c), namely the 241-, 782-, and 639-keV γ rays, a few other γ lines have been found to belong to the cascade, thanks to their coincidence relationships. The whole set forms two linked branches which are put on top of the 10^+ and 7^- states, respectively, since two parallel decay paths located just below the 241-keV transition, 557–1190 on the one hand and 253–661–1253 on the other hand, exactly fit the difference in energy between the 10^+ and 7^- isomeric states of ^{120}Sn (see Fig. 3). All the transitions newly observed in ^{120}Sn are given in Table II. The spin and parity of the new states will be discussed and assigned in Sec. III B5.

By using the data from the SAPhIR experiment, the transitions involved in the de-excitation of the 4890-keV level have been found to be delayed. The spectrum of γ rays

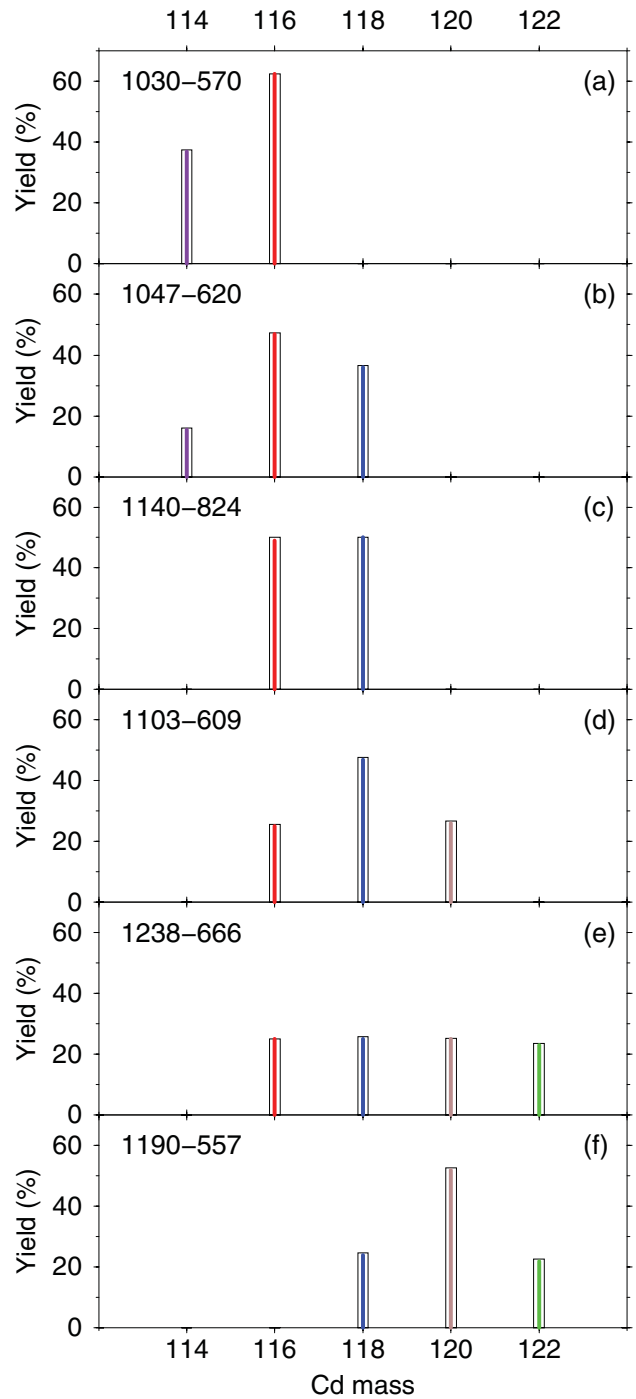

FIG. 2. (Color online) Relative yields of even-A Cd isotopes associated with the new γ-ray cascades emitted by the Sn isotopes produced in the ^{12}C + ^{238}U reaction. The yield of each even-A Cd isotope is computed from the number of counts of its $2^+ \rightarrow 0^+$ γ line in the spectra gated by the two strongest transitions of the new cascades (with their energies written in each drawing). (a) Case of the new cascade assigned to ^{126}Sn, (b) ^{124}Sn, (c) ^{123}Sn, (d) ^{122}Sn, (e) ^{121}Sn, and (f) ^{120}Sn. The new cascades assigned to ^{119}Sn and ^{125}Sn are discussed in Sec. III C1.

which have been detected in the time interval of 50 ns to 1 μs after the detection of two fragments by SAPhIR and

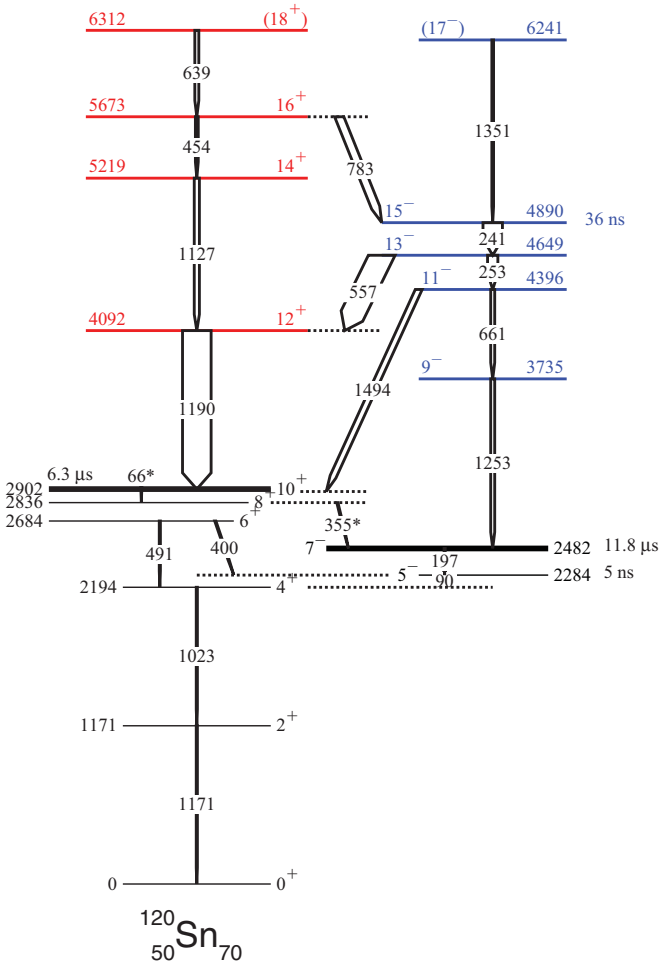

FIG. 3. (Color online) Level scheme of ^{120}Sn deduced in the present work. The colored levels are new. The two long-lived isomeric states [$T_{1/2} = 6.26(11)$ and 11.8(5) μs] and their γ decays to the low-lying states were already known [21]. The 355-keV transition, located between two long-lived isomeric states, as well as the very converted 66-keV transition, could not be observed in our work. The width of the arrows is representative of the relative intensity of the γ rays above the isomeric states.

in prompt coincidence with the 241/242-keV transition is drawn in Fig. 4(a). As this γ line is a triplet, the spectrum exhibits transitions emitted by the isomeric states of three fission fragments, ^{88}Rb [22], ^{120}Sn, and ^{122}Sn. The spectrum shown in Fig. 4(b) is gated by the 253-keV γ ray. This line is a doublet, as this energy occurs both in the decay of the 7^- isomeric state of ^{118}Sn (associated with the 1050- and 1230-keV transitions) and in the decay of the isomeric state at 4890 keV, newly established in ^{120}Sn. The statistics of this spectrum is too low to show the 1253-keV transition, identified in the thick-target Euroball experiment, from double-gated spectra having higher statistics.

The time distribution between the detection of two fragments by SAPhIR and the emission of the 1190-keV or the 557-keV γ ray is shown in Fig. 5(a). In order to reduce the background, we have selected the events containing an additional γ ray belonging to the 241–557–1190 cascade.

TABLE II. Properties of the new transitions assigned to ^{120}Sn in this experiment. The energies of the two long-lived isomeric states at 2481.6 keV ($I^\pi = 7^-$) and 2902.2 keV ($I^\pi = 10^+$) (listed in bold) are from Ref. [21].

E_γ (keV)[a]	I_γ [a,b]	$J_i^\pi \rightarrow J_f^\pi$	E_i (keV)	E_f (keV)
241.1(2)	95(14)	$15^- \rightarrow 13^-$	4890.1	4649.0
252.9(2)	36(7)	$13^- \rightarrow 11^-$	4649.0	4396.0
453.7(3)	9(3)	$16^+ \rightarrow 14^+$	5672.9	5219.3
556.5(2)	83(12)	$13^- \rightarrow 12^+$	4649.0	4092.5
639.0(3)	14(4)	$(18^+) \rightarrow 16^+$	6311.9	5672.9
661.1(3)	14(4)	$11^- \rightarrow 9^-$	4396.0	3734.6
782.8(3)	29(6)	$16^+ \rightarrow 15^-$	5672.9	4890.1
1127.0(4)	17(4)	$14^+ \rightarrow 12^+$	5219.3	4092.5
1190.3(3)	100	$12^+ \rightarrow 10^+$	4092.5	**2902.2**
1253.0(4)	14(4)	$9^- \rightarrow 7^-$	3734.6	**2481.6**
1350.8(5)	5(2)	$(17^-) \rightarrow 15^-$	6240.9	4890.1
1493.8(4)	22(5)	$11^- \rightarrow 10^+$	4396.0	**2902.2**

[a]The number in parentheses is the error in the last digit.
[b]The relative intensities are normalized to the sum $I_\gamma(557) + I_\gamma(1127) = 100$.

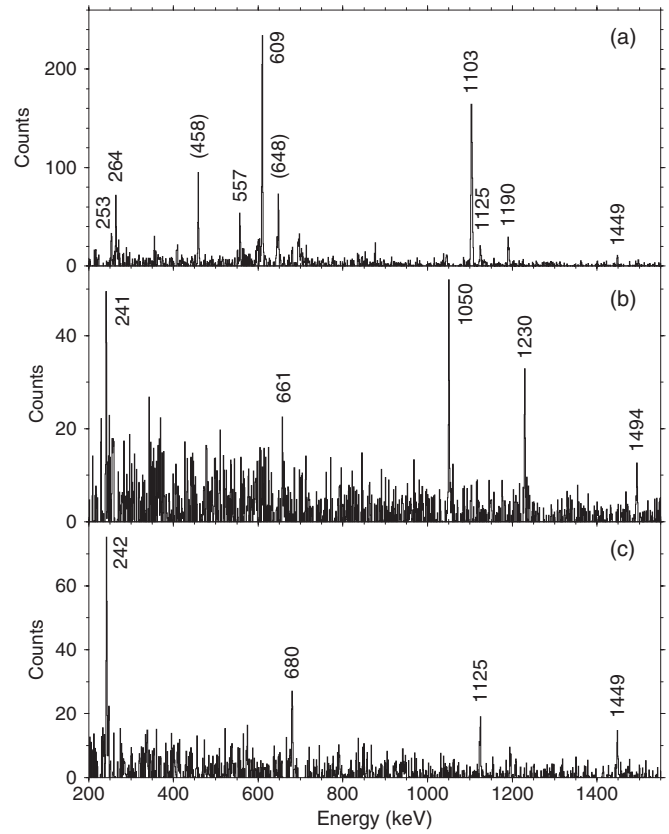

FIG. 4. Spectra of γ rays which have been detected in the time interval 50 ns–1μs after the detection of two fragments by SAPhIR. (a) γ rays in prompt coincidence with the 241/242 keV transition (^{120}Sn and ^{122}Sn). The 458- and 648-keV transitions are pollutions (belonging to the decay of the isomeric 7^+ state of ^{88}Rb [22]). (b) γ rays in prompt coincidence with the 253-keV transition, which is a doublet. The 1050- and 1230-keV γ rays are the first two transitions of ^{118}Sn and the 241-, 661-, and 1494-keV ones are assigned to ^{120}Sn. (c) γ rays in prompt coincidence with the 264 keV transition (^{122}Sn).

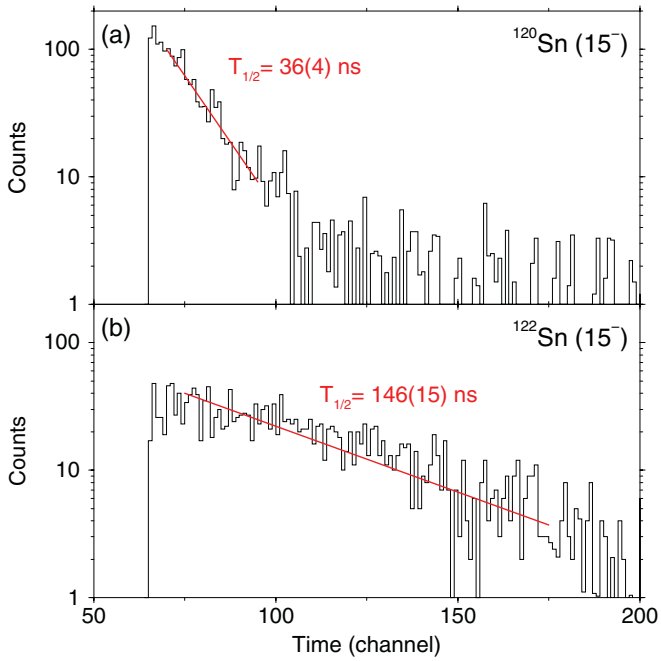

FIG. 5. (Color online) (a) Half-life of the 4890-keV state of ^{120}Sn obtained from the sum of the time distributions of the 1190- and 557-keV transitions. (b) Half-life of the 4720-keV state of ^{122}Sn obtained from the time distribution of the 1103-keV transition. See text for further details about the gating conditions and procedures.

Several least-squares fits of this spectrum were performed by varying the time interval from 70 to 100 ns and shifting the smallest intervals along the time axis. The average of all obtained values is $T_{1/2} = 36(4)$ ns, the adopted uncertainty being the observed dispersion (greater than the uncertainties quoted for each fit).

2. ^{122}Sn

For ^{120}Sn, the starting point is the two transitions at 1103 and 609 keV, which have to be placed above its long-lived isomeric states, because of the mass distribution of its partners in the two fusion reactions (Sec. III A). Several new transitions are observed in coincidence with the 1103- and 609-keV γ rays. All the observed relationships result in two linked branches which are placed above the the 10^+ and 7^- isomeric states of ^{122}Sn, since two parallel decay paths located just below the 242-keV transition, 609–1103 on the one hand and 264–680–1125 on the other hand, exactly fit their difference in energy (see Fig. 6). Examples of coincidence spectra of γ lines belonging to ^{122}Sn are given in Figs. 4(a) and 4(c), which demonstrate that all the transitions involved in the de-excitation of the 4720-keV level are delayed. The time distribution between the detection of two fragments by SAPhIR and the emission of the 1103-keV γ ray gives $T_{1/2} = 146(15)$ ns. In order to reduce the background we have selected the events containing either the 609-keV transition or the 242-keV one [see Fig. 5(b)].

All the transitions newly observed in ^{122}Sn are given in Table III. The spin and parity of the new states will be discussed and assigned in Sec. III B5.

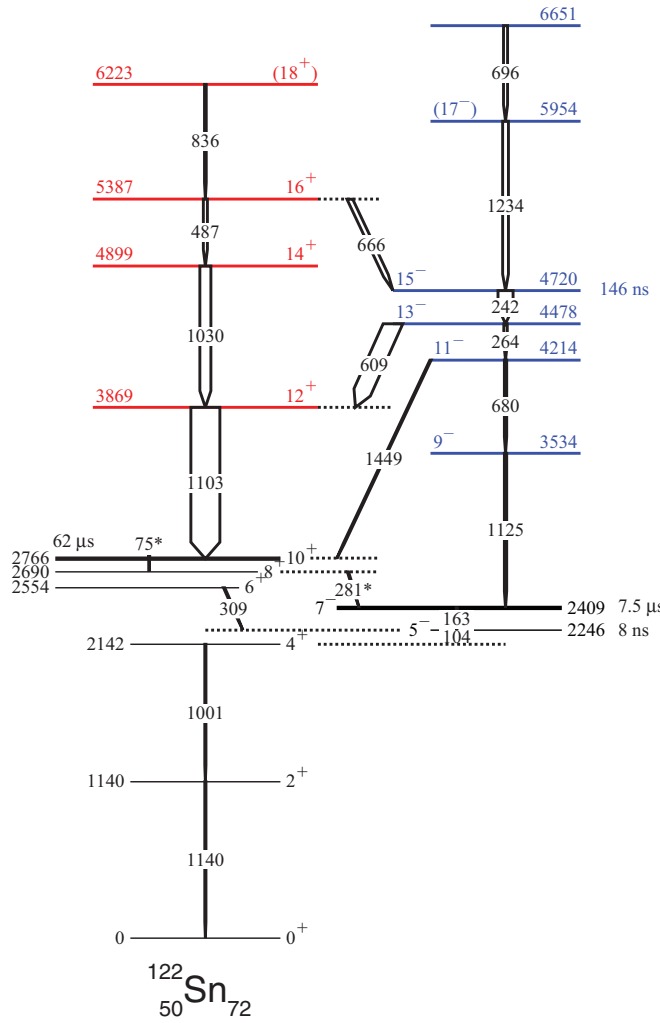

FIG. 6. (Color online) Level scheme of ^{122}Sn deduced in the present work. The colored levels are new. The two long-lived isomeric states [$T_{1/2} = 7.5(9)$ and $62(3)$ μs] and their γ decays to the low-lying states were already known [21]. The 281-keV transition, located between two long-lived isomeric states, as well as the very converted 75-keV transition, could not be observed in our work. The width of the arrows is representative of the relative intensity of the γ rays above the isomeric states.

3. ^{124}Sn

Similar procedures were used to identify the high-spin structures of ^{124}Sn. By gating on the two coincident transitions at 1047 and 620 keV assigned to ^{124}Sn because of the mass distribution of its partners in the two fusion reactions (Sec. III A), we found the 229- and the 1178-keV γ rays, establishing a cascade of four transitions. By using the data from the SAPhIR experiment, the first three transitions have been found to be delayed. The time distribution between the detection of two fragments by SAPhIR and the emission of the 1047- or the 620-keV γ ray gives $T_{1/2} = 260(25)$ ns. In order to reduce the background, we have selected the events containing an additional γ ray of the 229–620–1047 cascade. Since the 229–620–1047 sequence resembles well the 242–609–1103 sequence of ^{122}Sn and the 241–557–1190 one of ^{120}Sn, we

TABLE III. Properties of the new transitions assigned to ^{122}Sn in this experiment. The energies of the two long-lived isomeric states at 2409.0 keV ($I^\pi = 7^-$) and 2765.6 keV ($I^\pi = 10^+$) (listed in bold) are from Ref. [21].

E_γ (keV)[a]	I_γ [a,b]	$J_i^\pi \rightarrow J_f^\pi$	E_i (keV)	E_f (keV)
242.1(2)	52(9)	$15^- \rightarrow 13^-$	4720.5	4478.4
263.8(4)	11(3)	$13^- \rightarrow 11^-$	4478.4	4214.4
487.3(3)	14(4)	$16^+ \rightarrow 14^+$	5386.7	4899.4
609.3(2)	62(12)	$13^- \rightarrow 12^+$	4478.4	3869.1
665.9(3)	17(4)	$16^+ \rightarrow 15^-$	5386.4	4720.5
680.3(4)	7(3)	$11^- \rightarrow 9^-$	4214.4	3534.0
696.3(3)	14(4)	$\rightarrow (17^-)$	6650.8	5954.5
835.9(4)	6(3)	$(18^+) \rightarrow 16^+$	6222.6	5386.7
1030.3(3)	38(7)	$14^+ \rightarrow 12^+$	4899.4	3869.1
1103.5(3)	100	$12^+ \rightarrow 10^+$	3869.1	**2765.6**
1125.0(4)	7(3)	$9^- \rightarrow 7^-$	3534.0	**2409.0**
1234.0(4)	21(5)	$(17^-) \rightarrow 15^-$	5954.5	4720.5
1448.9(4)	4(2)	$11^- \rightarrow 10^+$	4214.4	**2765.6**

[a]The number in parentheses is the error in the last digit.
[b]The relative intensities are normalized to the sum $I_\gamma(609) + I_\gamma(1030) = 100$.

have placed the cascade of ^{124}Sn directly above its 10^+ state at 2657 keV excitation energy (see Fig. 7).

Moreover, we have identified other new transitions in ^{124}Sn by analyzing the spectra in double coincidence with the 1047-keV γ ray and one transition of its main complementary fragments (either ^{116,118}Cd or ^{96,98}Zr). An example of coincidence spectrum doubly-gated on some of the new transitions is shown in Fig. 8. The resulting cascade resembles well those assigned to the lighter isotopes, except for links such as the 666-keV transition (in ^{122}Sn) and the 783-keV one (in ^{120}Sn), which are no longer observed.

We have looked for a second branch directly linked to the 7^- isomeric state, as measured in ^{120,122}Sn. In the spectrum gated by the 229-keV line (SAPhIR experiment), a 252-keV transition is observed, as well as a weak 377-keV transition; these two transitions could be part of the foreseen cascade ending in the 7^- state. Unfortunately, no high-energy transition allowing us to complete the cascade could be unambiguously seen in that spectrum. Nevertheless, using the Euroball data sets, we identified a cascade of three transitions (253, 377, and 1116 keV) which does belong to ^{124}Sn since they are detected in coincidence with the complementary fragments expected in the two fusion reactions, namely ^{116,118}Cd and ^{96,98}Zr. Then we have assumed that the 253-keV transition measured in the present work is the one decaying the 8^+ state toward the 7^- isomeric state [21]. All these arguments would lead to a second decay path of the 4323-keV state, 252–377–1116–253. It is worth mentioning that the number of counts of the 253–1116–377 events measured in the Euroball data sets is very high compared to the very weak number of events containing the 252-keV transition located just above the 4071-keV state. This could be due to a large side feeding of that state. Since some intensities of the coincidence events establishing that second cascade are very weak, we have chosen to draw it with dotted lines in Fig. 7.

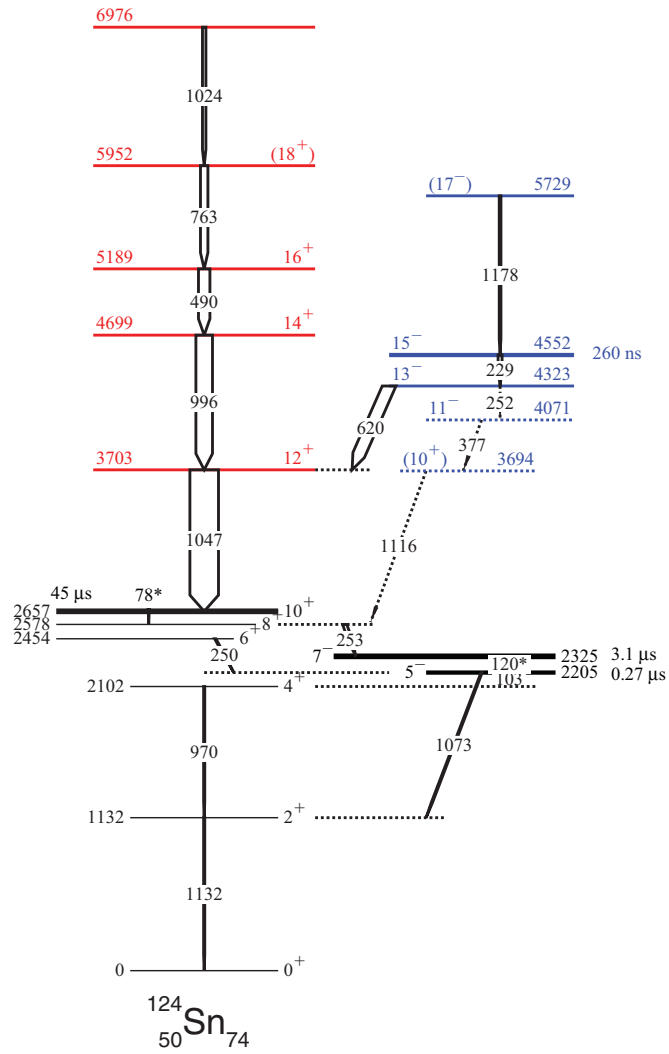

FIG. 7. (Color online) Level scheme of ^{124}Sn deduced in the present work. The colored levels are new. The two long-lived isomeric states [$T_{1/2} = 3.1(5)$ and 45(5) μs] and their γ decays to the low-lying states were already known [21]. The very converted 78- and 120-keV transitions could not be observed in our work. The width of the arrows is representative of the relative intensity of the γ rays above the isomeric states.

All the transitions newly observed in ^{124}Sn are given in Table IV. The spin and parity of the new states will be discussed and assigned in Sec. III B5.

4. ^{126}Sn

The two most intense transitions of the new cascade assigned to ^{126}Sn have energies of 1030 and 570 keV (see Sec. III A). The doubly-gated spectrum exhibits new transitions at 180, 1149, and 762 keV. Moreover, the data of the SAPhIR experiment indicate that the cascade comprising the first three transitions, at 1030, 570, and 180 keV, is delayed. Using the same procedures as previously described, we have measured the half-life, $T_{1/2} = 160(20)$ ns. Moreover, the spectrum doubly-gated by the 1030-keV line and one transition of a complementary fragment reveals other γ rays

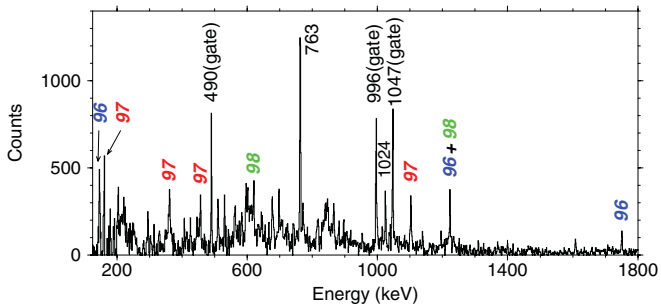

FIG. 8. (Color online) Coincidence spectrum double-gated on the 1047-, 996-, and 490-keV transitions of a new cascade identified in ^{124}Sn, built from the ^{18}O + ^{208}Pb data set. The γ rays emitted by the Zr complementary fragments are labeled by their masses A, written in italics.

belonging to ^{126}Sn, such as 986, 477, and 777 keV, which form another cascade. Thus ^{126}Sn exhibits two parallel structures having one transition in common, 1030 keV. In comparison to the results obtained in the lighter isotopes, we have placed it directly above the 10^+ isomeric state (see Fig. 9). Then we have looked for a second decay path of the new isomeric state ending in the 7^- state at 2219 keV, but we have found no candidate in our data sets. This is likely due to the lack of statistics, ^{126}Sn being in the heavy-A tail of the Sn fragment distribution.

Up to now, no 6^+ state was measured in ^{126}Sn, whereas such a state is expected to lie below the 8^+ state, as in the other even-A isotopes. The $E2$ decays of the 8^+_1 and 6^+_1 states are hindered because of their low energy, and thus these levels decay by means of E1 transitions toward negative-parity states 7^- and 5^-, respectively (see Figs. 6 and 7). In the present work, we have observed the $6^+_1 \rightarrow 5^-$ transitions of ^{120,122,124}Sn in coincidence with the first three transitions of their level schemes. Thus we have looked for the $6^+_1 \rightarrow 5^-$ γ ray in ^{126}Sn,

TABLE IV. Properties of the new transitions assigned to ^{124}Sn in this experiment. The energies of the two long-lived isomeric states at 2325.0 keV ($I^\pi = 7^-$) and 2656.6 keV ($I^\pi = 10^+$), as well as that of the 8^+ state (listed in bold) are from Ref. [21].

E_γ (keV)[a]	I_γ[a,b]	$J^\pi_i \rightarrow J^\pi_f$	E_i (keV)	E_f (keV)
228.5(4)	13(4)	$15^- \rightarrow 13^-$	4551.8	4323.2
251.7(4)	4(2)	$13^- \rightarrow 11^-$	4323.2	4071.4
253.2(3)	22(7)	$8^+ \rightarrow 7^-$	2578.4	**2325.0**
377.3(3)	7(3)	$11^- \rightarrow 9^-$	4071.4	3694.1
490.2(3)	39(6)	$16^+ \rightarrow 14^+$	5189.4	4699.2
619.8(2)	43(7)	$13^- \rightarrow 12^+$	4323.2	3703.4
762.7(3)	25(5)	$(18^+) \rightarrow 16^+$	5952.1	5189.4
995.8(3)	57(9)	$14^+ \rightarrow 12^+$	4699.2	3703.4
1024.3(4)	11(3)	$\rightarrow (18^+)$	6976.4	5952.1
1046.8(3)	100	$12^+ \rightarrow 10^+$	3703.4	**2656.6**
1115.7(3)	13(4)	$9^- \rightarrow 8^+$	3694.1	**2578.4**
1177.7(5)	5(2)	$(17^-) \rightarrow 15^-$	5729.4	4551.8

[a]The number in parentheses is the error in the last digit.
[b]The relative intensities are normalized to the sum $I_\gamma(996) + I_\gamma(620) = 100$.

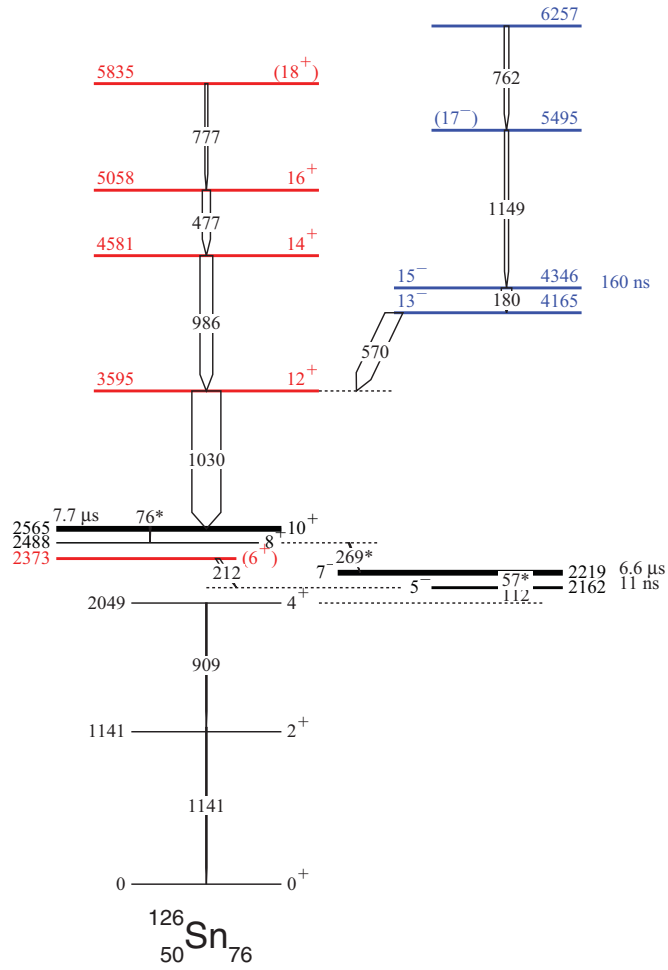

FIG. 9. (Color online) Level scheme of ^{126}Sn deduced in the present work. The colored levels are new. The two long-lived isomeric states and their γ decays to the low-lying states were already known [21]. The 269-keV transition, located between two long-lived isomeric states, as well as the very converted 76- and 57-keV transitions, could not be observed in our work. The width of the arrows is representative of the relative intensity of the γ rays above the isomeric states.

by analyzing the spectra doubly-gated by its first transitions (at 1141, 909, and 112 keV). Figure 10 shows two spectra, built from the ^{18}O + ^{208}Pb data set and using similar conditions for ^{126}Sn and ^{122}Sn. All the observed γ lines are assigned to the decay of known states of either ^{126}Sn (^{122}Sn) or their Zr complementary fragments, except the new γ line at 212 keV, which is assigned to the decay of the 6^+_1 state of ^{126}Sn (see Fig. 9).

Noteworthy is the fact that 212 keV is also the energy of the $2^+ \rightarrow 0^+$ transition of ^{100}Zr. The observation of prompt coincidence between a γ ray at this energy and the first transitions of ^{126}Sn could have been interpreted as the fact that ^{100}Zr is a complementary fragment of ^{126}Sn, meaning that the compound nucleus of the ^{18}O + ^{208}Pb reaction, ^{226}Th, may fission before emitting any neutrons. Such a process has never been observed, as expected since neutron emission from an excited compound nucleus is always faster than fission. The coincidence

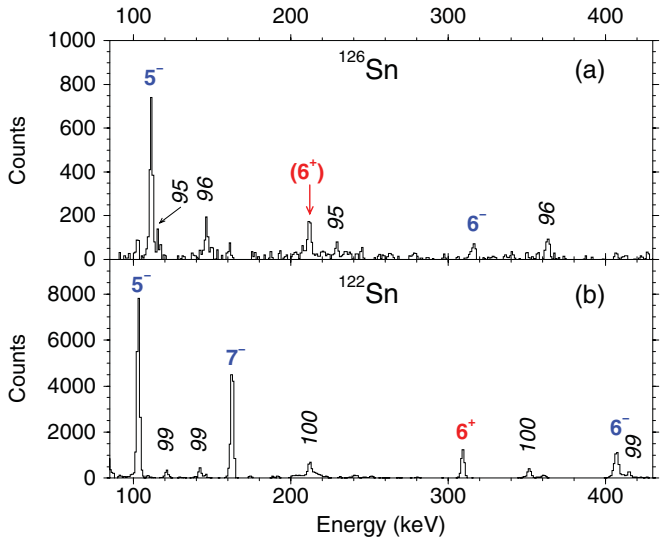

FIG. 10. (Color online) Coincidence spectra double-gated on the first two transitions of ^{126}Sn (a) and ^{122}Sn (b), built from the ^{18}O + ^{208}Pb data set. The γ rays emitted by ^{126,122}Sn are labeled by the spin and parity values of the decaying states, and those emitted by the Zr complementary fragments are labeled by their masses A, written in italics.

relationships measured in the ^{12}C + ^{238}U data set corroborate the location of the 212-keV γ line in the ^{126}Sn level scheme, which rules out a misinterpretation of the 212-keV γ line.

All the transitions newly observed in ^{126}Sn are given in Table V. The spin and parity of the new states will be discussed and assigned in Sec. III B5.

5. *Angular momentum and parity values of the high-spin states of $^{120-126}$Sn*

Given that the new high-spin structures of $^{120-126}$Sn reported in the previous sections are very close to each other, we assume that the similar states in the four level schemes have the same spin and parity values.

TABLE V. Properties of the new transitions assigned to ^{126}Sn in this experiment. The energies of the long-lived isomeric state at 2564.5 keV ($I^\pi = 10^+$) and of the 5^- state at 2161.5 keV (listed in bold) are from Ref. [21].

E_γ (keV)[a]	I_γ[a,b]	$J_i^\pi \rightarrow J_f^\pi$	E_i (keV)	E_f (keV)
180.5(3)	36(7)	$15^- \rightarrow 13^-$	4345.7	4165.2
211.7(4)	12(4)	$(6^+) \rightarrow 5^-$	2373.2	**2161.5**
476.7(3)	28(7)	$16^+ \rightarrow 14^+$	5057.9	4581.2
570.5(3)	56(11)	$13^- \rightarrow 12^+$	4165.2	3594.7
761.7(4)	8(3)	$\rightarrow (17^-)$	6256.9	5495.2
777.1(4)	9(3)	$(18^+) \rightarrow 16^+$	5835.0	5057.9
986.5(3)	44(9)	$14^+ \rightarrow 12^+$	4581.2	3594.7
1030.2(3)	100	$12^+ \rightarrow 10^+$	3594.7	**2564.5**
1149.5(5)	13(4)	$(17^-) \rightarrow 15^-$	5495.2	4345.7

[a]The number in parentheses is the error in the last digit.
[b]The relative intensities are normalized to the sum $I_\gamma(986) + I_\gamma(570) = 100$.

TABLE VI. Properties of the new isomeric states of $^{120-126}$Sn.

Nucleus	E_i (keV)	E_γ (keV)	$T_{1/2}$[a] (ns)	$B(E2)$[a] (e^2 fm^4)	$B(E2)$[a] (W.u.)
^{120}Sn	4890.1	241.1	36(4)	18(2)	0.51(5)
^{122}Sn	4720.5	242.1	146(15)	4.4(4)	0.12(1)
^{124}Sn	4551.8	228.5	260(25)	3.2(3)	0.09(1)
^{126}Sn	4345.7	180.5	160(20)	16(2)	0.42(5)

[a]The number in parentheses is the error in the last digit.

First, we have extracted the internal conversion coefficients of the isomeric transitions of $^{120-126}$Sn (at 241, 242, 229, and 180 keV, respectively) by analyzing the relative intensities of transitions in cascade. The intensity imbalances of the 241-, 242-, and 229-keV γ rays measured in spectra in double coincidence with at least one transition located above them in their respective level scheme lead to $\alpha_{tot} \leqslant 0.1$. This is consistent with an $E1$, $M1$, or $E2$ assignment. On the other hand, the intensity imbalance of the 180-keV γ ray of ^{126}Sn gives $\alpha_{tot} = 0.25(5)$, in good agreement with the theoretical value for $E2$ multipolarity, $\alpha_{tot}(E2, 180\,\text{keV}) = 0.20$ [23]. Assuming that the nature of the former transitions are also $E2$, we have calculated all the $B(E2)$ values, which are reported in Table VI. One has to note that these $B(E2)$ values have the same order of magnitude as those already measured for the isomeric decay of some lower energy states, either in the even-A isotopes or in the odd-A ones. This will be discussed in Sec. IV.

Second, we have analyzed the γ-γ angular correlations of strongest transitions. The experimental results are given in Table VII. The coincidence rates measured for six pairs indicate that all their transitions have the same multipole order: the 1190- and 241-keV transitions (in ^{120}Sn), the 1103-, 1030-, and 242-keV transitions (in ^{122}Sn), and the 1047-, 996-, and 490-keV transitions (in ^{124}Sn). Since the 241- and 242-keV transitions are $E2$, a quadrupole order is also assigned to the 1190-, 1103-, and 1030-keV transitions. Then the 1047-keV γ ray, located just above the 10^+ state of ^{124}Sn is also $E2$, as are the 1190- and 1103-keV γ rays in ^{120}Sn and ^{122}Sn, respectively. On the other hand, both the 557- and the 609-keV transitions have a

TABLE VII. Coincidence rates between γ rays of $^{120-124}$Sn as a function of their relative angle of detection, normalized to the ones obtained around 75°.

	E_γ-E_γ	$R(22°)$[a]	$R(46°)$[a]	$R(75°)$[a]
^{120}Sn	1190–557	0.87(9)	0.95(7)	1.00(5)
	1190–241	1.1(1)	1.12(8)	1.00(5)
^{122}Sn	1103–1030	1.17(9)	1.07(7)	1.00(5)
	1103–609	0.8(1)	0.96(7)	1.00(5)
	1103–242	1.2(1)	1.14(8)	1.00(5)
^{124}Sn	1047–996	1.15(9)	1.09(7)	1.00(5)
	1047–490	1.06(9)	1.11(7)	1.00(5)
	996–490	1.2(1)	1.05(7)	1.00(5)

[a]The number in parentheses is the error in the last digit.

different multipole order from that of the 1190- and 1103-keV transitions, respectively (see Table VII). Thus they are dipole transitions.

In conclusion, the cascades of three $E2$ transitions, placed above the 10^+ isomeric states of $^{120-126}$Sn, define the 12^+, 14^+, and 16^+ levels (see Figs. 3, 6, 7, and 9). Moreover, the second cascade identified in each level scheme comprises states with odd spin values: the $I = 13$ state decays to the 12^+ state and the $I = 15$ state is isomeric. A negative parity is assigned to the states of this second cascade since, in ^{120,122}Sn, the $I = 13$ state is linked to the long-lived 7^- state by means of a cascade of three transitions. This leads to the 9^- and 11^- states. All these assignments are reported in the level schemes drawn in Figs. 3, 6, 7, and 9.

6. *Comparison with other results recently published*

During the completion of this work, the decay of a new isomeric state in ^{128}Sn populated in the fragmentation of ^{136}Xe was reported [9]. Its de-excitation is very similar to that of the isomeric states we have measured in $^{120-126}$Sn. The spin and parity values of all the states involved in the isomeric decay were proposed by comparison with results of shell-model calculations.

Moreover, at the very end of the writing of this paper, we became acquainted with a publication on the high-spin states of the even-A $^{118-124}$Sn [24]. The authors have used the fusion-fission process to populate a few levels lying above the long-lived 10^+ states, the identification of the first transition of each γ-ray cascade being confirmed thanks to the behavior of its excitation function in the ^{124}Sn$(n, xn\gamma)$ reactions. The resulting four (three) new states of ^{120,124}Sn (^{122}Sn) are part of the structures identified in the present work.

C. Study of the odd-A Sn isotopes

Populated in deep inelastic reactions, a few medium-spin levels were identified in the four odd-A $^{119-125}$Sn isotopes prior to this work [3,6]. The maximum spin values measured in these isotopes were $27/2$ in case of negative parity and $19/2$ or $23/2$ in case of positive parity. Such states correspond to the breaking of one neutron pair in the $\nu h_{11/2}$ subshell, which gives rise to several sets of states, depending on the subshell occupied by the odd neutron. The $I^\pi = 27/2^-$ state, attributed to the $(\nu h_{11/2})^3$ configuration, is located between 3.1 and 2.6 MeV. It is a long-lived isomeric state in ^{123}Sn (34 μs), while the half-lives of the $27/2^-$ states of ^{119,121,125}Sn isotopes are in a 30- to 230-ns range, i.e., short enough such that coincidence events may be detected across the isomeric states. The maximum spin of the $(\nu h_{11/2})^2(\nu d_{3/2})$ configuration is $23/2^+$. Such a state, which is isomeric, is only known in ^{123,125}Sn. On the other hand, the four isotopes exhibit a long-lived isomeric $19/2^+$ state, from the $(\nu h_{11/2})^2(\nu s_{1/2})$ configuration, located around 2 MeV excitation energy.

Using the data of the two fusion-fission reactions of the present work, we have identified, for the first time, several structures of $^{119-125}$Sn located above 3 MeV excitation energy and spin values greater than $27/2$. In the following, we first present the building of each high-spin level scheme. Then, we discuss the angular momentum and parity assignments of most of the new states of $^{119-125}$Sn.

1. *^{119}Sn and ^{125}Sn*

The high-spin states of ^{119}Sn and ^{125}Sn are weakly populated in the two fusion-fission reactions used in the present work, as these two isotopes are in the tails of the Sn fragment distribution. The half-lives of their $27/2^-$ states (at 3101 and 2624 keV, respectively) are short enough to allow the detection of coincidence events across the isomers. Therefore the search for γ rays populating their $27/2^-$ states is more appropriate in the spectra gated by their low-lying transitions than in the spectra gated by their complementary fragments (namely $^{120-122}$Cd for ^{119}Sn and $^{114-116}$Cd for ^{125}Sn).

In both data sets registered in our work, all the spectra doubly-gated by the γ transitions decaying the $27/2^-$ state of ^{119}Sn reveal new γ lines which have to be placed above it (see Fig. 11). For ^{125}Sn, a cascade of three new γ transitions is observed in coincidence with the transitions decaying the $27/2^-$ state at 2624 keV (see Fig. 12). The new transitions of ^{119,125}Sn are also observed in spectra gated by γ rays emitted by their Cd partners. All the transitions observed in ^{119,125}Sn

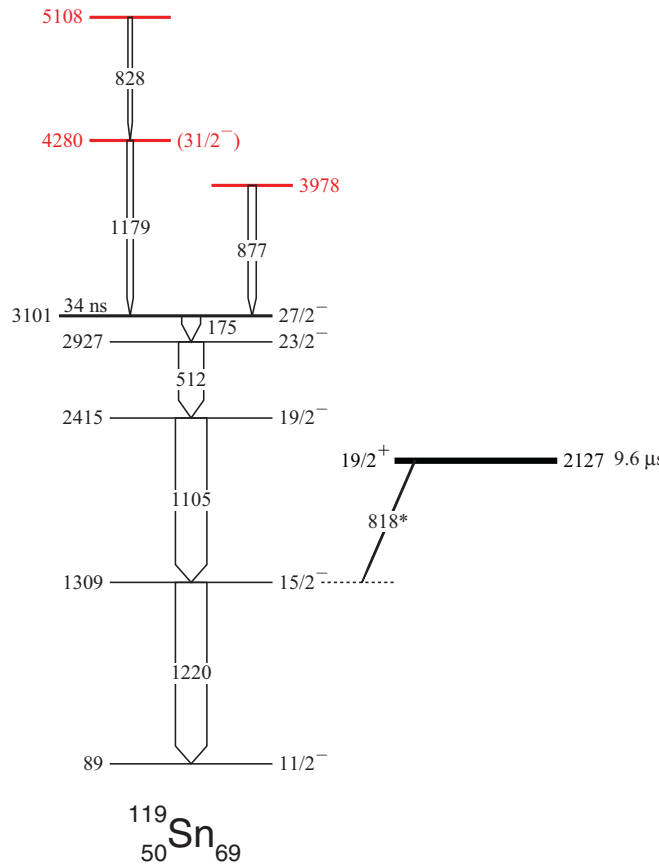

FIG. 11. (Color online) Level scheme of ^{119}Sn deduced in the present work. The colored levels are new. The width of the arrows is representative of the relative intensity of the γ rays. The two isomeric states were already known [21]. In our work, the 818-keV transition could not be observed; nevertheless, the $19/2^+$ isomeric state is drawn for the sake of completeness.

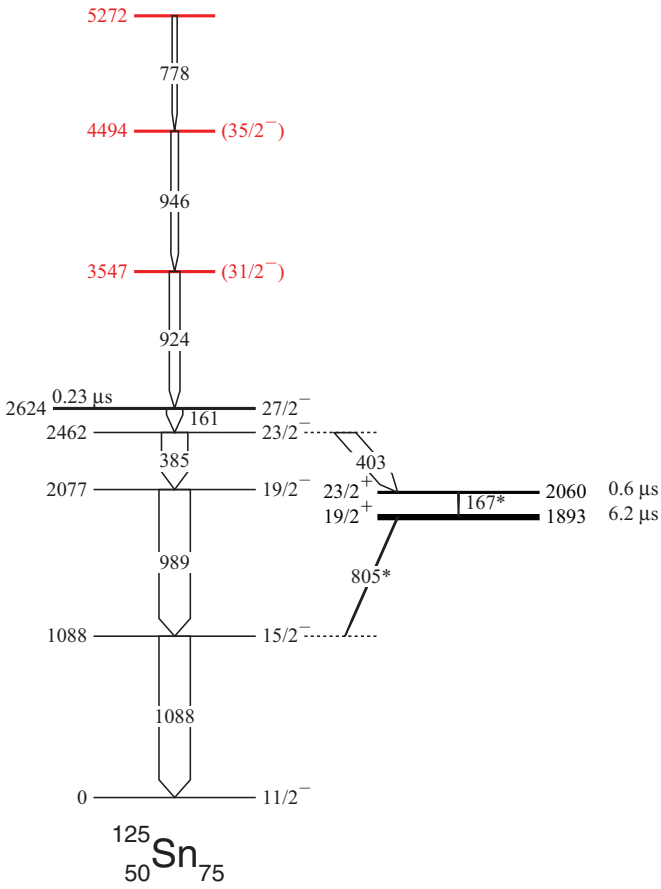

FIG. 12. (Color online) Level scheme of ^{125}Sn deduced in the present work. The colored levels are new. The width of the arrows is representative of the relative intensity of the γ rays. The three isomeric states were already known [21]. In our work, the 805-keV transition could not be observed and the very converted 167-keV line was extremely weak because of the lifetime of the decaying state.

are given in Tables VIII and IX, respectively. The spin and parity of the new states will be discussed in Sec. III C4.

We have not identified any γ-ray cascade which would be placed above the $19/2^+$ or $23/2^+$ states of ^{119}Sn or ^{125}Sn. Because of the long lifetime of these isomeric states, the transitions located above them can be only identified from their coincidences with transitions emitted by the partners. When taking into account that the weak population of these two Sn isotopes is shared among several complementary fragments, we found that every coincidence rate was too low in the present work.

TABLE VIII. Properties of the ^{119}Sn transitions. The excitation energy of the $11/2^-$ state (listed in bold) is from Ref. [21].

E_γ (keV)[a]	I_γ[a,b]	$J_i^\pi \rightarrow J_f^\pi$	E_i (keV)	E_f (keV)
174.6(3)	61(9)	$27/2^- \rightarrow 23/2^-$	3101.1	2926.6
511.9(3)	80(12)	$23/2^- \rightarrow 19/2^-$	2926.6	2414.7
827.8(4)	15(5)		5107.9	4280.1
876.8(4)	26(6)	$\rightarrow 27/2^-$	3977.9	3101.1
1105.2(3)	100	$19/2^- \rightarrow 15/2^-$	2414.7	1309.5
1179.0(5)	21(5)	$\rightarrow 27/2^-$	4280.1	3101.1
1220.0(3)	100	$15/2^- \rightarrow 11/2^-$	1309.5	**89.5**

[a]The number in parentheses is the error in the last digit.
[b]The relative intensities are normalized to $I_\gamma(1105) = 100$.

TABLE IX. Properties of the ^{125}Sn transitions.

E_γ (keV)[a]	I_γ[a,b]	$J_i^\pi \rightarrow J_f^\pi$	E_i (keV)	E_f (keV)
161.3(3)	51(8)	$27/2^- \rightarrow 23/2^-$	2623.3	2462.0
385.6(3)	84(12)	$23/2^- \rightarrow 19/2^-$	2462.0	2076.4
402.8(4)	52(12)	$23/2^- \rightarrow 23/2^+$	2462.0	2059.2
778.4(5)	16(5)		5271.9	4493.5
923.7(4)	34(8)	$\rightarrow 27/2^-$	3547.0	2623.3
946.5(4)	24(7)		4493.5	3547.5
988.7(3)	100	$19/2^- \rightarrow 15/2^-$	2076.4	1087.7
1087.7(3)	100	$15/2^- \rightarrow 11/2^-$	1087.7	0

[a]The number in parentheses is the error in the last digit.
[b]The relative intensities are normalized to $I_\gamma(989) = 100$.

2. ^{121}Sn

Prior to this work, knowledge of the medium-spin states of ^{121}Sn was very similar to that of ^{119}Sn, namely the $27/2^-$ and $19/2^+$ states and their decay toward the yrast levels having lower spin values. As in ^{119,125}Sn, the half-life of the $27/2^-$ isomer is short enough to measure the coincidence events across it. An example of a coincidence spectrum double-gated on the 1151-, 1030-, 470-, and 175-keV transitions of the yrast cascade is drawn in Fig. 13. Besides the transitions emitted by the complementary fragments, $^{100-98}$Zr, it exhibits new peaks at 1070, 1083, 1171, 1212, and 1457 keV. In a second step, we have analyzed the coincidence relationships of these new γ lines and placed all these transitions in three cascades above the $27/2^-$ state at 2833 keV (see Fig. 14). In addition, two other lines were observed in coincidence with a part of the yrast

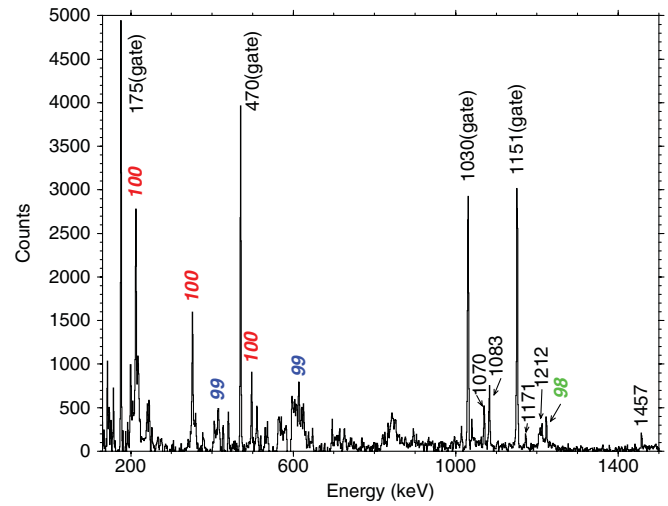

FIG. 13. (Color online) Coincidence spectrum double-gated on the 1151-, 1030-, 470-, and 175-keV transitions of the yrast cascade built on the low-lying $11/2^-$ state of ^{121}Sn produced in the ^{18}O + ^{208}Pb reaction. The γ rays emitted by the Zr complementary fragments are labeled by their masses A, written in italics.

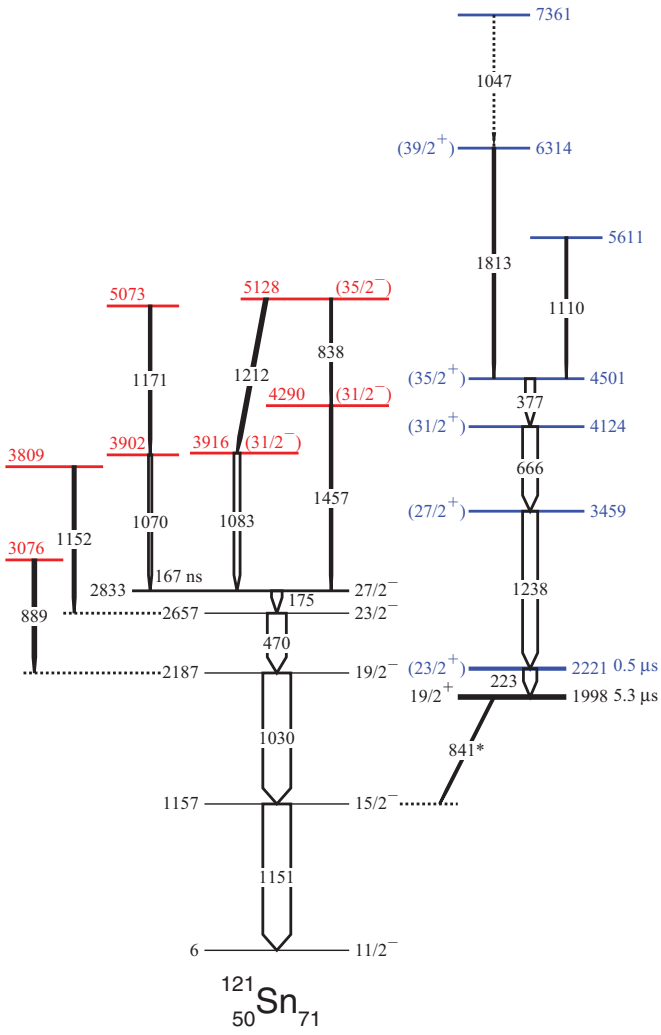

FIG. 14. (Color online) Level scheme of ^{121}Sn deduced in the present work. The colored levels are new. The isomeric $27/2^-$ and $19/2^+$ states and their decays were already known [21]. The 841-keV transition could not be observed in our work. The width of the arrows is representative of the relative intensity of the γ rays.

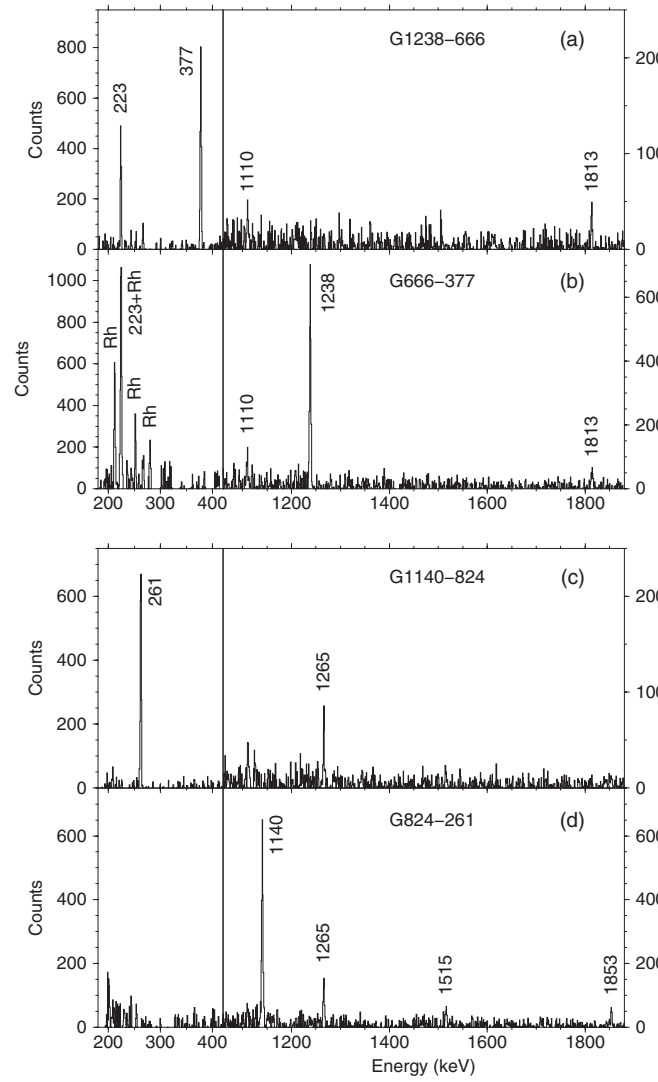

FIG. 15. Coincidence spectra double-gated on transitions belonging to two new cascades, built from the ^{12}C + ^{238}U data set, in two energy ranges, 180–420 keV and 1060–1880 keV. (a) and (b) Cascade emitted by ^{121}Sn. The lines labeled by Rh are pollutions (belonging to ^{111}Rh, the 667- and 378-keV transitions being part of its yrast cascade [25]). (c) and (d) Cascade emitted by ^{123}Sn.

transitions, and thus the 889-keV transition defines a new state at 3076 keV and the 1152-keV one a new state at 3809 keV.

The two most intense transitions of the new cascade assigned to ^{121}Sn thanks to their coincidences with their complementary fragments (see Sec. III A) have energies of 1238 and 666 keV. In the low-energy part of the double gate set on these two transitions [see Fig. 15(a)], two new transitions, at 223 and 377 keV, are clearly observed, the intensity of the 223-keV peak being the lowest. This would indicate that the 223-keV transition has to be located at the top of the cascade. Nevertheless, because of the comparison with the new cascade observed in ^{123}Sn (see Sec. III C3), we have chosen to put this transition at the bottom of the cascade, assuming that it de-excites an isomeric state with a half-life long enough to lower its relative intensity. The measured imbalance leads to $T_{1/2} = 0.5(1)$ μs when taking into account the conversion coefficient for an $E2$ transition, $\alpha_{\rm tot}(E2,\ 223\ {\rm keV}) = 0.096$ [23]. Unfortunately, the data from the SAPhIR experiment cannot be used to determine the half-life of this isomeric state, as it only emits one transition (in the time window of Euroball). The corresponding events contain a unique γ-ray, but this is not enough to select unambiguously the emitting nucleus.

In the high-energy part of the spectrum shown in Fig. 15(a), we observe two weak transitions, at 1110 and 1813 keV, which are also present in the spectrum doubly-gated by the 666- and 377-keV transitions [see Fig. 15(b)]. They are located at the top of the new cascade. Finally, the whole set is placed above the long-lived isomeric state at 1998 keV, which is the only solution to explain why these transitions do belong to the level scheme of ^{121}Sn while they are not detected in coincidence with its well-known yrast transitions.

All the transitions observed in ^{121}Sn are given in Table X. The spin and parity of the new states will be discussed in Sec. III C4.

TABLE X. Properties of the ^{121}Sn transitions. The excitation energies of the $11/2^-$ and $19/2^+$ states (listed in bold) are from Ref. [21]

E_γ (keV)[a]	I_γ [a,b]	$J_i^\pi \rightarrow J_f^\pi$	E_i (keV)	E_f (keV)
175.4(2)	38(9)	$27/2^- \rightarrow 23/2^-$	2832.7	2657.3
222.8(3)	48(10)[c]	$(23/2^+) \rightarrow 19/2^+$	2220.8	**1998.0**
376.9(3)	33(7)	$(35/2^+) \rightarrow (31/2^+)$	4501.2	4124.3
470.2(2)	68(13)	$23/2^- \rightarrow 19/2^-$	2657.3	2187.1
665.7(3)	53(11)	$(31/2^+) \rightarrow (27/2^+)$	4124.3	3458.6
837.8(4)	3(1)	$(35/2^-) \rightarrow (31/2^-)$	5128.0	4290.1
889.4(4)	9(3)	$\rightarrow 19/2^-$	3076.5	2187.1
1029.8(3)	100	$19/2^- \rightarrow 15/2^-$	2187.1	1157.3
1047.1(5)	weak	$\rightarrow (39/2^+)$	7361.3	6314.2
1069.7(4)	12(4)	$\rightarrow 27/2^-$	3902.4	2832.7
1082.9(4)	21(4)	$(31/2^-) \rightarrow 27/2^-$	3915.6	2832.7
1109.9(5)	4(3)	$\rightarrow (35/2^+)$	5611.1	4501.2
1151.0(3)	100	$15/2^- \rightarrow 11/2^-$	1157.3	**6.3**
1151.6(4)	8(4)	$\rightarrow 23/2^-$	3808.9	2657.3
1170.6(5)	6(3)		5073.0	3902.4
1212.5(4)	9(3)	$(35/2^-) \rightarrow (31/2^-)$	5128.0	3915.6
1237.8(3)	53(11)	$(27/2^+) \rightarrow (23/2^+)$	3458.6	2220.8
1457.4(4)	6(3)	$(31/2^-) \rightarrow 27/2^-$	4290.1	2832.7
1813.0(4)	5(2)	$(39/2^+) \rightarrow (35/2^+)$	6314.2	4501.2

[a]The number in parentheses is the error in the last digit.
[b]The relative intensities are normalized to $I_\gamma(1030) = 100$.
[c]See text.

3. ^{123}Sn

The $23/2^+$ and $27/2^-$ isomeric states were identified in ^{123}Sn, their very long half-lives being mainly due to the half-filling of the $\nu h_{11/2}$ subshell. Thus the identification of all its excited states with $I^\pi > 27/2^-$ or $23/2^+$ relies on the coincidences with γ rays emitted by its complementary fragments.

As for the previous cases, we start with the two coincident transitions at 1140 and 824 keV, assigned to ^{123}Sn because of the mass distribution of the complementary fragments in the two fusion-fission reactions (see Sec. III A). The low-energy part of the spectrum doubly-gated on these two transitions reveals one new γ line at 261 keV [see Fig. 15(c)] and the high-energy part of the spectrum doubly-gated on the 261- and 824-keV transitions shows new high-energy, low-intensity transitions [see Fig. 15(d)].

The resulting structure, which is very similar to the one assigned to ^{121}Sn, is placed above the positive-parity isomeric state, the $23/2^+$ state at 2153 keV (see Fig. 16). It is worth noting that, due to the time range defining the coincidence events (about 300 ns), the already-known $E2$ transition (208 keV) de-exciting this long-lived state ($T_{1/2} = 6\mu$s) is never included in an event registered in our experiment. This explains why the new structure of ^{123}Sn contains one low-energy transition (261 keV) instead of the two transitions (223 and 377 keV) observed in ^{121}Sn, as discussed in the previous section. Noteworthy is the fact that the three transitions decaying the 4378-keV state of ^{123}Sn have not been measured in the SAPhIR experiment. Thus the half-life of this state is smaller than 30 ns.

In addition, several weak transitions were observed in coincidence with those emitted by the same partners as ^{123}Sn (namely ^{116,118}Te and ^{98}Zr). They form two cascades of three γ rays in mutual coincidences, which look like the new cascade of ^{125}Sn (located on the top of the $27/2^-$ state because of the coincidence relationships with its yrast transitions; see Fig. 12). Thus we have tentatively placed the two new cascades above the long-lived $27/2^-$ state of ^{123}Sn (see Fig. 16).

All the transitions observed in ^{123}Sn are given in Table XI. In our experiments, a small number of events which contain the low-lying transitions of ^{123}Sn are registered since the prompt fold of the corresponding cascades is strongly lowered by the long half-life of the $27/2^-$ state (34 μs). Thus the intensities of the transitions located below that state could not be given relative to that of the ones located above the isomeric states. Nevertheless, we have chosen to put the γ lines in Table XI, as their energies are now known more precisely than previously [3]. The spin and parity of the new states will be discussed in Sec. III C4.

4. Angular momentum and parity values of the high-spin states of $^{119-125}$Sn

The statistics of our data related to the high-spin states of the odd-A Sn nuclei is too low to perform γ-γ angular correlation analyses. Therefore, the spin assignments shown in Figs. 11, 12, 14, and 16 are based upon a few features:

(i) All the transitions with an energy $\gtrsim$1 MeV are assumed to have an $E2$ multipolarity.
(ii) The 223-keV transition of ^{121}Sn is assumed to be $E2$ (see Sec. III C2).
(iii) The 666- and 377-keV transitions of ^{121}Sn, as well as the 824- and 261-keV transitions of ^{123}Sn, are assumed to be $E2$, as the $35/2^+$ state with the $(\nu h_{11/2})^4(\nu d_{3/2})^1$ configuration is expected to decay to the $23/2^+$ state

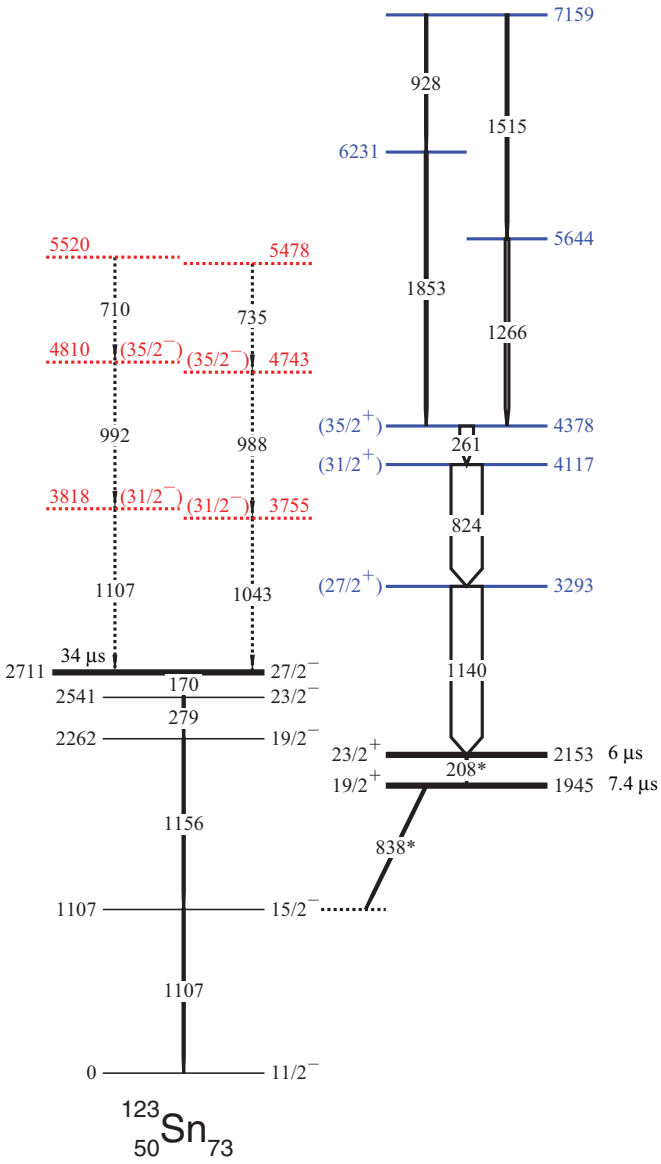

FIG. 16. (Color online) Level scheme of ^{123}Sn deduced in the present work. The colored levels are new. The isomeric $27/2^-$, $23/2^+$, and $19/2^+$ states and their decays were already known [21]. The 208- and 838-keV transitions could not be observed in our work. as well as several other decays of the $27/2^-$ and $23/2^-$ states [3]. Two new cascades are tentatively placed above the $27/2^-$ state (see text). The width of the arrows is representative of the relative intensity of the γ rays, except for that of the decay of the $27/2^-$ long-lived isomeric state (see text).

with the $(\nu h_{11/2})^2(\nu d_{3/2})^1$ configuration by means of a cascade of three $E2$ transitions.

Lastly, we can compute a few transition probabilities. As mentioned above, the half-life of the 2221-keV state of ^{121}Sn is $T_{1/2} = 0.5(1)$ μs, then the value of $B(E2; 23/2^+ \rightarrow 19/2^+)$ is 1.9(4) e^2 fm^4. The half-life of the 4378-keV state of ^{123}Sn is $T_{1/2} < 30$ ns, which leads to the value of the reduced transition probability, $B(E2; 35/2^+ \rightarrow 31/2^+) > 15$ e^2 fm^4.

TABLE XI. Properties of the ^{123}Sn transitions. The excitation energy of the $23/2^+$ state (listed in bold) is from Ref. [21].

E_γ (keV)[a]	I_γ[a,b]	$J_i^\pi \rightarrow J_f^\pi$	E_i (keV)	E_f (keV)
169.8(2)	[c]	$27/2^- \rightarrow 23/2^-$	2711.3	2541.5
261.4(3)	43(9)	$(35/2^+) \rightarrow (31/2^+)$	4378.0	4116.6
279.1(2)	[c]	$23/2^- \rightarrow 19/2^-$	2541.5	2262.4
823.6(3)	100	$(31/2^+) \rightarrow (27/2^+)$	4116.6	3293.0
928.3(4)	3(1)	$\rightarrow (39/2^+)$	7159.2	6231.0
1106.8(2)	[c]	$15/2^- \rightarrow 11/2^-$	1106.8	0
1140.0(3)	100	$(27/2^+) \rightarrow 23/2^+$	3293.0	**2153.0**
1155.6(2)	[c]	$19/2^- \rightarrow 15/2^-$	2262.4	1106.8
1265.8(4)	12(4)	$\rightarrow (35/2^+)$	5643.8	4378.0
1515.3(5)	6(2)		7159.2	5643.8
1853.0(5)	5(2)	$(39/2^+) \rightarrow (35/2^+)$	6231.0	4378.0
710.5(3)	[d]		5520.4	4809.9
735.0(3)	[d]		5477.6	4742.6
987.8(3)	[d]	$(35/2^-) \rightarrow (31/2^-)$	4742.6	3754.8
991.6(3)	[d]	$(35/2^-) \rightarrow (31/2^-)$	4809.9	3818.3
1043.5(3)	[d]	$(31/2^-) \rightarrow 27/2^-$	3754.8	2711.3
1107.0(3)	[d]	$(31/2^-) \rightarrow 27/2^-$	3818.3	2711.3

[a]The number in parentheses is the error in the last digit.
[b]The relative intensities are normalized to $I_\gamma(824) = 100$.
[c]See text.
[d]Tentative attribution.

IV. DISCUSSION

A. General features of j^n configurations

The nuclear shell model (SM) describes the many-body nuclear system in terms of a single-particle Hamiltonian representing the average effect of the strong nucleon-nucleon interactions on a given nucleon plus residual interactions among a smaller number of particles, the valence nucleons near the Fermi surface, $H = H_0 + V_{\rm res}$. The identification of states involving many identical nucleons in the same orbit j, i.e., states with the j^n configuration, is a straightforward application of SM. These states are expected to exhibit typical features indicating properties of the residual interaction. For instance, it is now well known that, when it is assumed that only two-body forces contribute, $V_{\rm res}(1, 2)$, the interaction between n nucleons in one shell j, can be expressed in terms of the two-particle matrix elements. Moreover, when using the seniority number, v (which can be defined as the number of unpaired nucleons[2]), we can relate the two-body interaction matrix elements of seniority-v states in the j^n configuration to the matrix elements in the j^v configuration.

To illustrate these features, it is instructive to look at results of calculations performed many years ago on the proton $(h_{11/2})^n$ configurations [27]. The spectra associated with $n = 3$, 4, 5, and 6, the latter corresponding to midshell,[3] were calculated using the residual interactions taken from the

[2]For a recent review on the use of the seniority quantum number in many-body systems, see Ref. [26].

[3]Due to particle-hole symmetry, the spectrum associated with the $(\pi h_{11/2})^n$ configuration is the same as the $(\pi h_{11/2})^{12-n}$ one. Thus it is sufficient to discuss the cases with $n \leqslant 6$.

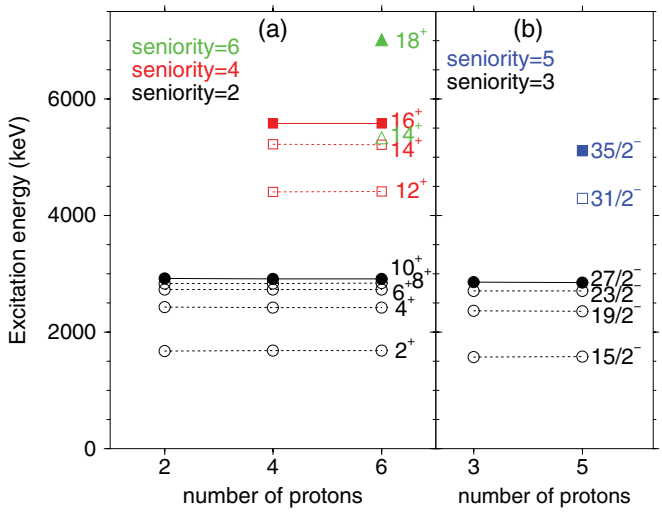

FIG. 17. (Color online) Evolution of the yrast states with the $(\pi h_{11/2})^n$ configuration as a function of n, the number of protons occupying the orbit (see text). (a) Even number of protons. The states with one broken pair ($v = 2$) are drawn in black, with two broken pairs ($v = 4$) in red and three broken pairs ($v = 6$) in green. (b) Odd number of protons. The states with one broken pair ($v = 3$) are drawn in black, with two broken pairs ($v = 5$) in blue.

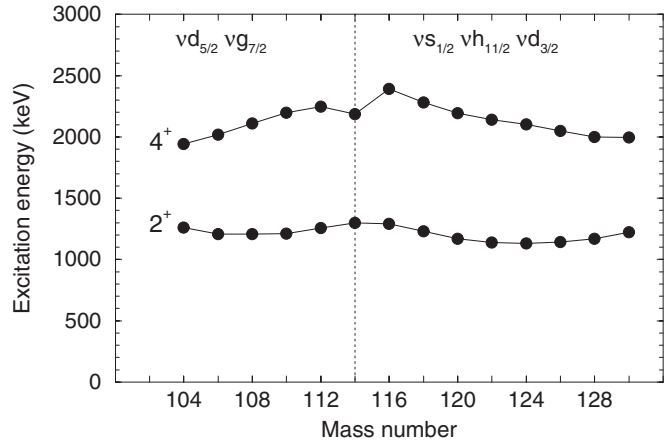

FIG. 18. Evolution of the 2_1^+ and 4_1^+ states of the Sn isotopes, as a function of the mass number.

experimental spectrum of $^{148}_{66}\mathrm{Dy}_{82}$ (with $n = 2$). For $n \geqslant 3$, there are often several states with the same angular momentum. If the two-body residual interactions conserve seniority, the latter can be used as a quantum number to characterize each state. It is worth recalling that, to be diagonal in the seniority scheme, a condition involving the five diagonal matrix elements of the $(h_{11/2})^2$ interaction has to be fulfilled [28]. While this condition is not satisfied by most general two-body interactions, it is fulfilled in the present case [27]. Thus the predicted spectra of $(h_{11/2})^n$ configurations are very similar, whatever the number of nucleons.

This is illustrated by the theoretical results obtained for the yrast states of $(\pi h_{11/2})^n$ configurations with even n, drawn in Fig. 17(a). Above the first multiplet ($I^\pi = 2^+, \ldots, 10^+$) of $v = 2$ seniority, we observe a second group of states ($I^\pi = 12^+$, 14^+, and 16^+) with $v = 4$. When breaking a third $h_{11/2}$ pair, we obtain the highest-spin value available in this orbit, $I^\pi = 18^+$. It is worth noting that the $v = 6$ 14^+ state is located below the $v = 4$ 16^+ state, which has a paramount importance for the decay of the 16^+ state. While the $16^+ \rightarrow 14_2^+$ transition is allowed, the one between states of the same seniority is forbidden as the orbit is half-filled, i.e., $B(E2; 16^+ \rightarrow 14_1^+) = 0$. As a result, the value of the half-life of the 16^+ state of the $(\pi h_{11/2})^6$ configuration can be even lower than the one of the 16^+ state of the $(\pi h_{11/2})^4$ configuration.

The results obtained for the yrast states of $(\pi h_{11/2})^n$ configurations with odd n are drawn in Fig. 17(b). While the energy of the $27/2^-$ state is close to the one of the 10^+ state, the highest-spin states obtained for an odd number of nucleons are located at lower energy than the ones obtained for an even number. Thus we expect a more compressed spectrum when the number of nucleons occupying the j orbit is odd.

Unfortunately, the experimental behaviors of the $(\pi h_{11/2})^{4,5,6}$ configurations have never been tested, the nuclei of interest lying very close to the proton drip line. Since they are only produced in reactions with very low cross sections, their high-spin states could not be identified.

Pure j^n configurations occur in a very few nuclei, since an orbit j is rarely bounded by two gaps in energy. The closeness of several orbits leads to configuration mixings; nevertheless, some of the features due to seniority are found to survive. For instance, there are in semi-magic nuclei fairly constant spacings between the 0^+ ground state and some $v = 2$ states, even though large changes in configuration mixings occur. The Sn nuclei provide a typical example; the energies of their first two states ($I^\pi = 2^+$ and 4^+) do not vary much across the major shell ($54 < N < 80$), while the neutron orbits evolve from $[\nu d_{5/2}, \nu g_{7/2}]$ for $N < 64$ to $[\nu s_{1/2}, \nu h_{11/2}, \nu d_{3/2}]$ for $N > 64$ (see Fig. 18).

The highest-spin states of the Sn isotopes with $N > 64$ do contain a large $(\nu h_{11/2})^n$ component, since the two low-j orbits cannot afford large spin values. Therefore their study as a function of the neutron number gives us the opportunity to explore the main features of the $(\nu h_{11/2})^{4,5,6}$ configurations. However, such a work is restricted to $A \geqslant 120$ since the yrast states of the lightest-A Sn isotopes are dominated by a collective band coming from two-particle–two-hole excitations across the $Z = 50$ gap, which hampers identifying states coming from the $(\nu h_{11/2})^n$ configurations. The maximum values of angular momentum obtained for various configurations with several broken pairs are given in Table XII.

B. High-seniority states of the Sn isotopes

The systematics of the excitation energies of the highest-spin states in the $^{120-128}$Sn even-A isotopes are shown in Fig. 19. Noteworthy is the fact that the highest-energy state of ^{122,126}Sn measured in the present work is assigned to be the 19^- state, which is expected above the 17^- state, given that the $19^- – 17^-$ distance in energy is most likely lower than that of the $17^- – 15^-$ one.

TABLE XII. Various configurations with several broken pairs expected in heavy-A Sn isotopes.

Configuration	$I^{\pi}_{\max}$	Nucleus
$(\nu h_{11/2})^2$	10^+	even A
$(\nu h_{11/2})^3$	$27/2^-$	odd A
$(\nu h_{11/2})^4$	16^+	even A
$(\nu h_{11/2})^5$	$35/2^-$	odd A
$(\nu h_{11/2})^6$	18^+	even A
$(\nu h_{11/2})^1(\nu d_{3/2})^1$	7^-	even A
$(\nu h_{11/2})^2(\nu d_{3/2})^1$	$23/2^+$	odd A
$(\nu h_{11/2})^3(\nu d_{3/2})^1$	15^-	even A
$(\nu h_{11/2})^4(\nu d_{3/2})^1$	$35/2^+$	odd A
$(\nu h_{11/2})^5(\nu d_{3/2})^1$	19^-	even A
$(\nu h_{11/2})^6(\nu d_{3/2})^1$	$39/2^+$	odd A

The evolution of the positive-parity states is very smooth. Likewise, the energies of the negative-parity states display a very regular behavior. This indicates that their main configurations are the same, whatever the number of neutrons. Being very close in energy for $69 \leqslant N \leqslant 81$, the three neutron orbits $(\nu s_{1/2}, \nu h_{11/2}, \nu d_{3/2})$ are gradually filled together. Then the occupation number of the $\nu h_{11/2}$ subshell does not change by two units from one even-A isotope to the next one and the maximum value of seniority does not display the stepwise behavior as a function of A, shown in Fig. 17.

By taking into account the maximum values of angular momentum given in Table XII, it is tempting to assume that the positive-parity states have the $(\nu h_{11/2})^4$ and $(\nu h_{11/2})^6$ configurations and that the negative-parity states have the $(\nu h_{11/2})^3(\nu d_{3/2})^1$ and $(\nu h_{11/2})^5(\nu d_{3/2})^1$ configurations. Nevertheless, we can notice immediately the peculiar behavior of the 18^+ states: (i) the irregular variation of its excitation energy as a function of A and (ii) the low value of the 18^+–16^+ gap in energy compared to the results given in Fig. 17. Thus the main configuration of the 18^+ states is likely not the h^6 configuration (which will be discussed in the next section). All the assignments written in Fig. 19 are corroborated by the results of shell-model calculations presented in Sec. IV C.

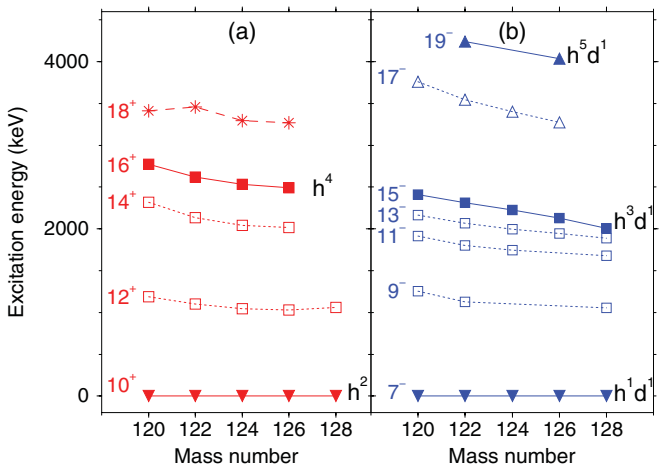

FIG. 19. (Color online) Evolution of the highest-spin states of the even-A Sn isotopes, as a function of the mass number (this work and Ref. [9] for ^{128}Sn). The state having the maximum angular momentum of each configuration is drawn with a filled symbol. (a) Excitation energies of the positive-parity states above the 10^+ level. For the peculiar behavior of the 18^+ states (drawn with asterisks), see text. (b) Excitation energies of the negative-parity states above the 7^- level.

As above mentioned, when using the proton $h^2_{11/2}$ residual interactions extracted from the ^{148}Dy spectrum, the 14^+ state with seniority $v = 6$ is located below the 16^+ state with seniority $v = 4$. Then the 16^+ state decays predominantly toward the 14^+_2 state when the subshell is half-filled, since the decay toward the 14^+_1 state is hindered. For the Sn isotopes, we did not observe any delayed component in the γ-ray cascades located below the 16^+ states, meaning that their half-lives are smaller than 30 ns. This would lead to $B(E2; 16^+ \rightarrow 14^+) > 0.7\ e^2\ \mathrm{fm}^4$ for ^{124}Sn, for instance. This limit is close to the low value of $B(E2; 10^+ \rightarrow 8^+)$ in ^{122,124}Sn, which is due to the half-filling of the $\nu h_{11/2}$ orbit [3] (see below). Thus in order to determine whether the 14^+ states measured in the Sn isotopes have seniority $v = 4$ or $v = 6$, we would need to know a more precise limit of the 16^+ half-lives.

The $E2$ decays of the isomeric 15^- states identified in the even-A $^{120-126}$Sn isotopes allow us to confirm their main configuration, $(\nu h_{11/2})^3(\nu d_{3/2})^1$. It is well known that the sign of the $E2$ transition amplitude between two states with the same seniority depends on the occupation rate of the orbit, being positive for low values and negative for high values. Thus the behavior of $\sqrt{B(E2; 10^+ \rightarrow 8^+)}$ as a function of the Sn mass number was used to determine the half-filling of the $\nu h_{11/2}$ orbit, i.e., when particle and hole contributions exactly cancel one another. That happens for $A = 123$ or $N = 73$ [3]. Results obtained in odd-A Sn isotopes corroborated this value [4,7]. Indeed the transition probability between two states with seniority $v = 3$, such as $B(E2; 27/2^- \rightarrow 23/2^-)$, displays the same behavior with regard to the orbit filling as the one between two states with seniority $v = 2$, such as $B(E2; 10^+ \rightarrow 8^+)$. Nevertheless, in order to plot the $\sqrt{B(E2)}$ values of both the even- and odd-A Sn isotopes in the same graph, one has to compensate for the fractional parentage coefficients entering in the expression of the states with seniority $v = 3$ [28]: the $B(E2)$ values corresponding to $v = 3$ have to be multiplied by 0.264 [29].

The $E2$ transition amplitudes for these two sets of isomeric transitions, as well as the results of the $15^- \rightarrow 13^-$ transitions obtained in the present work, are drawn in Fig. 20. This last set follows exactly the same trend as those of the $10^+ \rightarrow 8^+$ transitions and the $27/2^- \rightarrow 23/2^-$ ones. This confirms that the main configuration of the 15^- and 13^- states of the even-A $^{120-126}$Sn isotopes is $(\nu h_{11/2})^3(\nu d_{3/2})^1$.

The excitation energies of the negative-parity states above the $27/2^-$ level in $^{119-125}$Sn are drawn in Fig. 21(a). The highest-spin states of seniority $v = 5$ are more compressed in energy than the ones of seniority $v = 4$ shown in Fig. 19(a), as predicted for the $(\pi h_{11/2})^n$ configuration (see Sec. IV A and Fig. 17).

The positive-parity states above the $23/2^+$ level in ^{121}Sn and ^{123}Sn are due to the breaking of two and three neutron pairs in the $\nu h_{11/2}$ orbit [see Fig. 21(b)]. Their almost-constant energies indicate once more that the three neutron orbits close

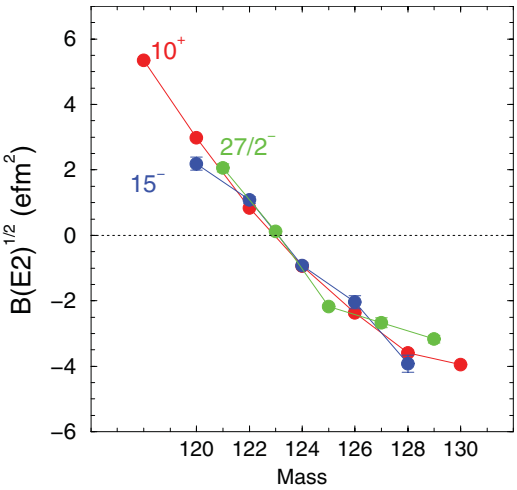

FIG. 20. (Color online) $E2$ transition amplitudes for the $(\nu h_{11/2})^n$ isomeric transitions in the Sn isotopes, with $n = 2$ for the decay of the 10^+ states and $n = 3$ for the decays of the $27/2^-$ and 15^- states. The experimental values for the $27/2^-$ states (in green) and for the 15^- states (in blue) have been normalized (see text).

to the Fermi level are gradually filled, so the level energies do not depend very much on the total number of neutrons.

C. Results of shell-model calculations

We have performed shell-model calculations using the ANTOINE code [30], the calculational details being the same as those described in Ref. [31]. Since the present work mainly involves high-spin states, we have restricted the calculations to the excited states with spin values higher than $7^-/10^+$ for the even-A isotopes and $23/2^+/27/2^-$ for the odd-A isotopes.

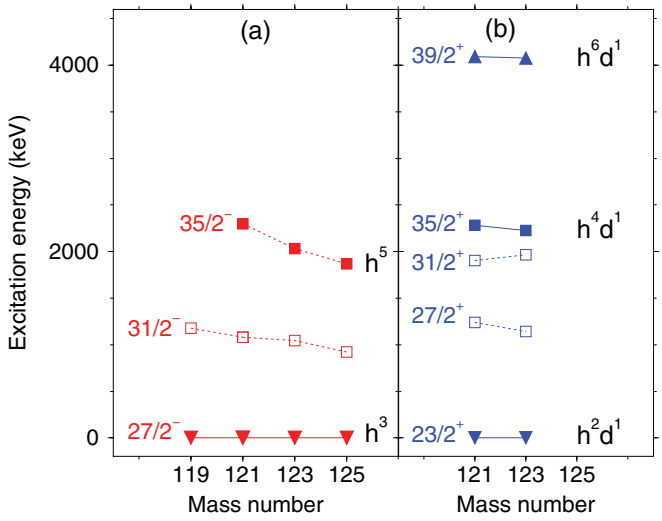

FIG. 21. (Color online) Evolution of the highest-spin states of the odd-A Sn isotopes, as a function of the mass number (this work). The state having the maximum angular momentum of each configuration is drawn with a filled symbol. (a) Excitation energies of the negative-parity states above the $27/2^-$ level. (b) Excitation energies of the positive-parity states above the $23/2^+$ level.

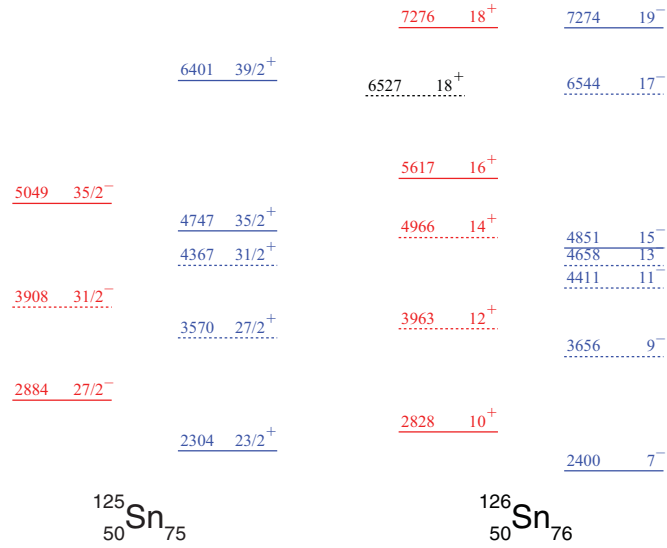

FIG. 22. (Color online) High-spin levels of ^{125}Sn and ^{126}Sn predicted by the SM calculations (see text).

In this section, we only present results of ^{125}Sn and ^{126}Sn, as those of the lower-A isotopes are nearly the same.

The yrast spectra above the long-lived isomeric states are shown in Fig. 22. The angular momenta of the states drawn with dotted lines comprise components involving a broken pair in the low-j orbits, $\nu d_{3/2}$ or $\nu s_{1/2}$. The comparison of results given in Fig. 22 with those obtained for a pure $(h_{11/2})^n$ configuration (see Fig. 17) shows the influence of the low-j neutron orbits in the energies of these states. For instance, the $31/2^-$ state is now located at mid-distance between the $35/2^-$ and the $27/2^-$ states (see Fig. 22). In the same manner, the 12^+ state is located at mid-distance between the 14^+ and the 10^+ states, while it is located nearer the 14^+ state in the first calculation.

On the other hand, the states drawn with solid lines are due to the complete alignment of the $h_{11/2}$ momenta of the neutron belonging to the broken pairs (cf. the configurations given in Table XII). For instance, the main configuration of the $35/2^+$ state of ^{125}Sn is $(\nu s_{1/2})^0(\nu d_{3/2})^3(\nu h_{11/2})^8$ (61%), i.e., the breaking of two $\nu h_{11/2}$ pairs, and the main configuration of the $39/2^+$ state is $(\nu s_{1/2})^2(\nu d_{3/2})^3(\nu h_{11/2})^6$ (79%), i.e., the breaking of three $\nu h_{11/2}$ pairs. Results obtained for ^{126}Sn are very similar, except for the 18^+ yrast state (drawn in black in Fig. 22). Its main configuration is $(\nu s_{1/2})^1(\nu d_{3/2})^3(\nu h_{11/2})^8$ (59%), the $(\nu s_{1/2})^2(\nu d_{3/2})^4(\nu h_{11/2})^6$ component being considerably weaker (11%). Conversely, the main component of the 18^+_2 state (drawn in red in Fig. 22) is $(\nu s_{1/2})^2(\nu d_{3/2})^4(\nu h_{11/2})^6$ (79%), i.e., the breaking of three $\nu h_{11/2}$ pairs. Thus in ^{126}Sn, the breaking of the third $\nu h_{11/2}$ pair, which only provides an angular momentum of $2\hbar$, competes unfavorably with the breaking of a low-j pair, which can also provide an angular momentum of $2\hbar$, either from the $(\nu s_{1/2})^1(\nu d_{3/2})^3$ configuration or from the $(\nu d_{3/2})^2$ one. It is worth noting that such a process does not occur in the $39/2^+$ state of ^{125}Sn, because of the blocking of the $\nu d_{3/2}$ orbit by the odd neutron.

These theoretical results are in good agreement with the experimental ones; in particular, the various distances in

energy between successive states are well reproduced. First, the 14^+–12^+ distance is found to be close to the 12^+–10^+ one, as measured experimentally. Similar results are obtained for the $35/2^-$–$31/2^-$ and $31/2^-$–$27/2^-$ spacings, which are well predicted. Second, the bunching of the three states with $I^\pi = 11^-$, 13^-, and 15^-, as well as the large gap between the 15^- and 17^- states, is well reproduced. Lastly, the peculiar behavior of the experimental 18^+ states is likely due to the breaking of a low-j neutron pair, which is expected to evolve as a function of A since the $\nu s_{1/2}$ orbit gets farther away from the neutron Fermi level as N is increasing.

In summary, we have identified states having the maximum value of angular momentum of either the $(\nu h_{11/2})^n$ configurations or the $(\nu h_{11/2})^n(\nu d_{3/2})^1$ ones, with $n = 1$, 2, 3, 4, 5, and 6, in the even-A and odd-A Sn isotopes (see Table XII and also Figs. 19 and 21). The only missing state is the 18^+ state from the $(\nu h_{11/2})^6$ configuration, which is not yrast.

D. Search for high-seniority states from other j^n configurations

While there are numerous examples of states with seniority $v = 2$ in the literature, states with seniority $v = 4$ are scarce. The 10^+ and 12^+ states of the $(\pi g_{9/2})^4$ configuration have been identified in the two $N = 50$ isotones, ^{94}Ru and ^{96}Pd [21]. On the other hand, the highest-spin level measured in the $(\nu g_{9/2})^4$ configuration (^{72,74}Ni$_{44,46}$) is the 8^+ state of seniority $v = 2$. As for the $(\pi h_{11/2})^n$ configuration, which is expected in the $N = 82$ isotones having $Z \geqslant 68$, only one experimental result has been obtained as the nuclei of interest are close to the proton drip line: The $v = 4$ 16^+ state of the $(\pi h_{11/2})^4$ configuration is identified in $^{150}_{68}$Er [21].

The next high-j orbital is $i_{13/2}$, which is located in the middle of the 82–126 major shell. The excitation energy of the $13/2^+$ state measured in ^{199,201}Pb is around 500 keV above the $5/2^-$ and $3/2^-$ states, meaning that the main configurations of the high-spin states expected in the Pb isotopes are likely complex. Indeed, several $v = 4$ states, which were measured in the ^{200,202,204}Pb nuclei [21], have the configurations $(\nu i_{13/2})^2(\nu f_{5/2})^2$ (16^+) and $(\nu i_{13/2})^3(\nu f_{5/2})^1$ $(17^-, 19^-)$, but the breaking of two or three pairs of $i_{13/2}$ neutrons has never been observed. We have to recall that the high-spin level schemes of these Pb nuclei display coexisting collective structures, which makes it difficult to identify the states having $(\nu i_{13/2})^n$ configuration, with $n > 3$.

In the Sn nuclei, several high-spin states having a configuration j^v, with $v = 5$ and 6, are identified for the first time in the present work. Such an observation is unique in the whole nuclear chart, because several prerequisites are needed which seem to be only fulfilled by the heavy-A Sn nuclei and the $\nu h_{11/2}$ orbit: (i) the nuclei have to be spherical, without shape coexistence leading to a vast number of high-spin states forming the yrast sequence, (ii) the spherical high-j orbit has to be isolated from the others in order to be the main active one, and (iii) the high-spin states of the nuclei of interest have to be populated with enough intensity to be measured.

V. SUMMARY AND CONCLUSION

Thanks to the high efficiency of the Euroball array, many high-spin states have been identified in $^{119-126}$Sn isotopes. These nuclei have been produced as fission fragments in two reactions induced by heavy ions: ^{12}C + ^{238}U at 90 MeV bombarding energy and ^{18}O + ^{208}Pb at 85 MeV. The level schemes have been built up to 5–7 MeV excitation energy by analyzing triple γ-ray coincidence data. Spin and parity values have been assigned to most of the high-spin states using γ-γ angular correlation results. In addition, the use of the fission-fragment detector, SAPhIR, has allowed us to identify new isomeric states in the even-A $^{120-126}$Sn isotopes. All the observed states can be described in terms of several broken neutron pairs occupying the $\nu h_{11/2}$ orbit. The maximum value of angular momentum available in this high-j shell, i.e., for its midoccupation and the breaking of the three pairs (seniority $v = 6$), has been identified.

This process, which is observed for the first time in spherical nuclei, has some similarities to the one involved in some deformed nuclei. Several $N = 90$ isotones show evolution of collectivity with spin. While the nuclei are prolate for $I = 0$, the lowest-energy states at $I = 40$–50 are due to oblate shape. There the nuclei can be considered as a closed core of ^{146}Gd and several additional valence particles in the j orbits lying above the $Z = 64$ and $N = 82$ closures. Then the observed band structure terminates at the maximum value of spin available to the valence nucleons. For instance, in $^{158}_{68}$Er, band termination occurs at spin $46\hbar$ [32], when all the 12 valence nucleon spins are aligned, $(\pi h_{11/2})^4(\nu f_{7/2})^3(\nu h_{9/2})^3(\nu i_{13/2})^2$, i.e., a configuration with six broken pairs but involving four different orbits.

ACKNOWLEDGMENTS

The Euroball project was a collaboration among France, the United Kingdom, Germany, Italy, Denmark, and Sweden. The first experiment has been performed under U.E. Contract No. ERB FHGECT 980 110 at Legnaro. The second one has been supported in part by the EU under Contract No. HPRI-CT-1999-00078 (EUROVIV). We thank many colleagues for their active participation in the experiments: A. Bogachev, A. Buta, J. L. Durell, Th. Ethvignot, F. Khalfalla, I. Piqueras, A. A. Roach, A. G. Smith and B. J. Varley. We thank the crews of the tandem of Legnaro and of the Vivitron, as well as M.-A. Saettle for preparing the Pb target and P. Bednarczyk, J. Devin, J.-M. Gallone, P. Médina, and D. Vintache for their technical help during the second experiment. We are indebted to K. Sieja and F. Nowacki for providing us with their effective nucleon-nucleon interactions.

[1] J. Bron *et al.*, Nucl. Phys. A **318**, 335 (1979).
[2] P. J. Daly *et al.*, Z. Phys. A **323**, 245 (1986).
[3] R. H. Mayer *et al.*, Phys. Lett. B **336**, 308 (1994).
[4] R. Broda *et al.*, Phys. Rev. Lett. **68**, 1671 (1992).

[5] J. A. Pinston *et al.*, Phys. Rev. C **61**, 024312 (2000).
[6] C. T. Zhang, P. Bhattacharyya, P. J. Daly, Z. W. Grabowski, R. Broda, B. Fornal, and J. Blomqvist, Phys. Rev. C **62**, 057305 (2000).
[7] R. L. Lozeva *et al.*, Phys. Rev. C **77**, 064313 (2008).
[8] B. Fogelberg, K. Heyde, and J. Sau, Nucl. Phys. A **352**, 157 (1981).
[9] S. Pietri *et al.*, Phys. Rev. C **83**, 044328 (2011).
[10] J. Simpson, Z. Phys. A **358**, 139 (1997).
[11] J. Eberth *et al.*, Nucl. Instrum. Methods A **369**, 135 (1996).
[12] G. Duchêne *et al.*, Nucl. Instrum. Methods A **432**, 90 (1999).
[13] D. Radford, Nucl. Instrum. Methods A **361**, 297 (1995).
[14] Ch. Theisen *et al.*, AIP Conf. Proc. **447**, 143 (1998).
[15] M. A. C. Hotchkis *et al.*, Nucl. Phys. A **530**, 111 (1991).
[16] M. G. Porquet *et al.*, Acta Phys. Pol. B **27**, 179 (1996).
[17] M. Houry *et al.*, Eur. Phys. J. A **6**, 43 (1999).
[18] M. Houry, Ph.D. thesis, Université Paris XI, Orsay, 2000.
[19] R. Lucas *et al.*, Eur. Phys. J. A **15**, 315 (2002).
[20] M. G. Porquet, Int. J. Mod. Phys. E **13**, 29 (2004).
[21] ENSDF database, [http://www.nndc.bnl.gov/ensdf/].
[22] M. G. Porquet *et al.*, Eur. Phys. J. A **40**, 131 (2009).
[23] T. Kibédi *et al.*, Nucl. Instrum. Methods A **589**, 202 (2008).
[24] N. Fotiades *et al.*, Phys. Rev. C **84**, 054310 (2011).
[25] Ts. Venkova *et al.*, Eur. Phys. J. A **15**, 429 (2002).
[26] P. Van Isacker, AIP Conf. Proc. **1323**, 141 (2010).
[27] R. D. Lawson, Z. Phys. A **303**, 51 (1981).
[28] I. Talmi, *Simple Models of Complex Nuclei* (Harwood Academic, Reading, MA, 1993), Chaps. 15 and 20.
[29] J. H. McNeill *et al.*, Phys. Rev. Lett. **63**, 860 (1989).
[30] E. Caurier and F. Nowacki, Acta Phys. Pol. B **30**, 705 (1999).
[31] K. Sieja, F. Nowacki, K. Langanke, and G. Martínez-Pinedo, Phys. Rev. C **79**, 064310 (2009).
[32] P. O. Tjom, R. M. Diamond, J. C. Bacelar, E. M. Beck, M. A. Deleplanque, J. E. Draper, and F. S. Stephens, Phys. Rev. Lett. **55**, 2405 (1985).